



山东科技大学

SHANDONG UNIVERSITY OF SCIENCE AND TECHNOLOGY

本科毕业设计（论文）

荣乌柳泉中桥方案设计与结构计算

**Scheme design and calculation of Liuquan Medium bridge on
Rongwu highway**

学 院：_____ 土木工程与建筑学院

专业班级：_____ 土木工程留学生 2021 级

姓 名：_____ WINDI RAHMASARI

学 号：_____ 202111051662

指导教师：_____ 焦玉颖


完成日期：_____ 2025 年 06 月 10 日

教务处制

学位论文原创性声明

本人呈交给山东科技大学的学位论文，除所列参考文献和世所公认的文献外，全部是本人攻读学位期间在导师指导下的研究成果。除文中已经标明引用的内容外，本论文不包含任何其他个人或集体已经发表或撰写过的研究成果。对本文的研究做出贡献的个人和集体，均已在文中以明确方式标明。本人完全意识到本声明的法律结果由本人承担。

若有不实之处，本人愿意承担相关法律责任。

本人签名： 


日期：2025 年 06 月 10 日

学位论文使用授权声明

本人完全了解山东科技大学有关保留、使用学位论文的规定，同意本人所撰写的学位论文的使用授权按照学校的管理规定处理。

作为申请学位的条件之一，学校有权保留学位论文并向国家有关部门或其指定机构送交论文的电子版和纸质版；有权将学位论文的全部或部分内容编入有关数据库发表，并可以以电子、网络及其他数字媒体形式公开出版；允许学校档案馆和图书馆保留学位论文的纸质版和电子版，可以使用影印、缩印或扫描等复制手段保存和汇编学位论文；为教学和科研目的，学校档案馆和图书馆可以将公开的学位论文作为资料在档案馆、图书馆等场所或在校园网上供校内师生阅读、浏览。

（保密的学位论文在解密后适用本授权）

作者签名： 

导师签名： 焦玉颖

日期：2025 年 06 月 10 日

日期：2025 年 06 月 10 日

毕业论文（设计）检测系统

文本复制检测报告单 (全文标明引文)

№:BC20250529195820224216798

检测时间:2025-05-29 19:58:20

篇名: Scheme design and calculation of Liuquan Medium bridge on Rongwu highway
 作者: WINDI RAHMASARI (202111051662)
 指导教师: 焦玉颖
 检测机构: 山东科技大学
 文件名: 202111051662-WINDI RAHMASARI CIVIL ENGINEERING 2021.pdf
 检测系统: 毕业论文（设计）检测系统（毕业论文（设计）管理系统）
 检测类型: 毕业论文设计
 检测范围: 中国学术期刊网络出版总库
 中国博士学位论文全文数据库/中国优秀硕士学位论文全文数据库
 中国重要会议论文全文数据库
 中国重要报纸全文数据库
 中国专利全文数据库
 图书资源
 优先出版文献库
 大学生论文联合比对库
 互联网资源(包含贴吧等论坛资源)
 英文数据库(涵盖期刊、博硕、会议的英文数据以及德国Springer、英国Taylor&Francis 期刊数据库等)
 港澳台学术文献库
 互联网文档资源
 源代码库
 CNKI大成编客-原创作品库
 时间范围: 1900-01-01至2025-05-29

检测结果

去除本人文献复制比: 12.9%
 跨语言检测结果: -

去除引用文献复制比: 12.9%
 总文字复制比: 12.9%

单篇最大文字复制比: 7.6% (Scheme Design and Structural Calculation of Chayuan middle-span bridge on Rongwu Highway)

重复字数: [14539]
 总段落数: [7]

总字数: [112429]
 疑似段落数: [7]

单篇最大重复字数: [8542]
 前部重合字数: [1554]

疑似段落最大重合字数: [5127]
 后部重合字数: [12985]

疑似段落最小重合字数: [160]

文字复制部分 12.9%
 引用部分 0%
 无问题部分 87.1%

指标: ☐ 疑似剽窃观点 ☒ 疑似剽窃文字表述 ☐ 疑似整体剽窃 ☐ 过度引用

相似表格: 0 相似公式: 没有公式 疑似文字的图片: 0

| | | |
|-------------|-------------|---|
| 9.5%(1554) | 9.5%(1554) | Scheme design and calculation of Liuquan Medium bridge on Rongwu highway_第1部分 (总16334字) |
| 4.9%(788) | 4.9%(788) | Scheme design and calculation of Liuquan Medium bridge on Rongwu highway_第2部分 (总16096字) |
| 14.2%(2365) | 14.2%(2365) | Scheme design and calculation of Liuquan Medium bridge on Rongwu highway_第 |

3部分 (总16709字)

Scheme design and calculation of Liuquan Medium bridge on Rongwu highway_第4部分 (总16007字)

Scheme design and calculation of Liuquan Medium bridge on Rongwu highway_第5部分 (总16548字)

Scheme design and calculation of Liuquan Medium bridge on Rongwu highway_第6部分 (总16388字)

Scheme design and calculation of Liuquan Medium bridge on Rongwu highway_第7部分 (总14347字)

(注释: 无问题部分 文字复制部分 引用部分)

1. Scheme design and calculation of Liuquan Medium bridge on Rongwu highway_第1部分 总字数: 16334

相似文献列表

| | | |
|---|---|------------------------|
| 去除本人文献复制比: 9.5%(1554) 去除引用文献复制比: 9.5%(1554) 文字复制比: 9.5%(1554) 疑似剽窃观点: (0) | | |
| 1 | Scheme design and calculation of Wangcun Middle-span bridge on Rongwu freeway M. FAREL ASHROFIE - 《大学生论文联合比对库》- 2024-06-26 | 6.3% (1030) 是否引证: 否 |
| 2 | Scheme design and calculation of Xiaoxin River Middle-span bridge on Rongwu highway YERIBU PROSPER AWOLEBA - 《大学生论文联合比对库》- 2024-07-02 | 4.1% (668) 是否引证: 否 |
| 3 | Scheme Design and Structural Calculation of Chayuan middle-span bridge on Rongwu Highway NAURA BERLIAN HUMAIROH - 《大学生论文联合比对库》- 2024-06-14 | 3.7% (611) 是否引证: 否 |
| 4 | 桥梁与隧道工程英文简介.ppt 全文免费 - 《网络 (https://max.book118.)》- 2024 | 0.6% (95) 是否引证: 否 |

原文内容

本科毕业设计 (论文)
荣乌高速柳泉中桥方案设计与结构计算
Scheme design and calculation of Liuquan Medium bridge on Rongwu highway
学院: 土木工程与建筑学院
专业班级: 土木工程留学生2021级
姓名: WINDI RAHMASARI
学号: 202111051662
指导教师: 焦玉颖完成日期: 2025年05月29日
教务处制
学位论文原创性声明
本人呈交给山东科技大学的学位论文, 除所列参考文献和世所公认的文献外, 全部是本人攻读学位期间在导师指导下的研究成果。除文中已经标明引用的内容外, 本论文不包含任何其他个人或集体已经发表或撰写过的研究成果。对本文的研究做出贡献的个人和集体, 均已在文中以明确方式标明。本人完全意识到本声明的法律结果由本人承担。
若有不实之处, 本人愿意承担相关法律责任。
本人签名: 日期: 2025年05月29日
学位论文使用授权声明
本人完全了解山东科技大学有关保留、使用学位论文的规定, 同意本人所撰写的学位论文的使用授权按照学校的管理规定处理。
作为申请学位的条件之一, 学校有权保留学位论文并向国家有关部门或其指定机构送交论文的电子版和纸质版; 有权将学位论文的全部或部分内容编入有关数据库发表, 并可以以电子、网络及其他数字媒体形式公开出版; 允许学校档案馆和图书馆保留学位论文的纸质版和电子版, 可以使用影印、缩印或扫描等复制手段保存和汇编学位论文; 为教学和科研目的, 学校档案馆和图书馆可以将公开的学位论文作为资料在档案馆、图书馆等场所或在校园网上供校内师生阅读、浏览。
(保密的学位论文在解密后适用本授权)
作者签名:
日期: 2025年05月29日
导师签名:
日期: 2025年05月29日

摘要

本桥梁设计基于荣乌高速刘泉中桥的地质勘察数据，涵盖了方案比选、上部结构设计分析以及后期养护与维修策略的专项研究。设计工作的主要内容包括：

1. 设计参数：本桥按照一级公路荷载标准设计，桥面布置为双车道，每道宽度为 10.75米，总桥宽为21.50米。桥梁采用两跨布置，每跨长度为21米。抗震设防等级为B类，地基土层为粉质黏土。

2. 方案比选：对几种桥梁结构方案进行了评估，包括开放式拱桥，预应力空心板桥以及钢筋混凝土简支梁桥。通过全面的比较分析，最终确定钢筋混凝土简支梁桥为最佳方案。

3. 结构设计与分析：上部结构采用T型梁截面形式。设计内容包括纵向高程布置，通过横向荷载分布系数与荷载组合效应确定关键参数，以及钢筋的合理布置。对主梁进行内力分析，并验证其抗弯性能，抗剪能力以及挠度是否满足规范要求。此外，设计还包括横隔板布置，钢筋结构细节及桥面铺装连续性的详细计算。

4. 专题研究：基于深度学习算法的检测工具已被开发，用于识别桥面板上的裂缝。该技术通过自动化裂缝识别过程，显著提升了养护工作的准确性和效率。

关键词：公路桥梁简支T形梁，上部结构，内力计算，AutoCAD.

ABSTRACT

The bridge design is informed by geological data from the Liuquan Medium Bridge on Rongwu Highway and encompasses scheme selection, structural analysis for both the superstructure, as well as a focused study on maintenance and repair strategies. Major components of the design include :

1. Design Criteria : The bridge is designed to accommodate Class I Highway Loads and features two lanes, each 10.75 meters wide, resulting in a total bridge width of 21.50 meters. It consists of two spans, each measuring 21 meters. The seismic design falls under category B, with a foundation layer composed of silty clay.

2. Scheme Evaluation : Several bridge structure alternatives were evaluated, such as the open spandrel arch type, the prestressed hollow slab design, and the simply supported beam bridge utilizing reinforced concrete. Following a thorough comparison, the reinforced concrete beam bridge was determined to be most effective and suitable choice.

3. Structural Design and Analysis : The T-beam cross-sectional form is adopted for the superstructure configuration. The design process encompasses vertical alignment planning, the calculation of critical design parameters through lateral load distribution coefficients and load combination effect, as well as a systematic arrangement of reinforcement bars. Structural analysis was conducted to assess internal forces acting on the main beams, followed by validation of flexural strength, shear resistance, and deflection compliance. Furthermore, the design integrates thorough calculations related to diaphragm placement, reinforcement detailing, and surface layer continuity.

4. Special Research : A software application utilizing deep learning algorithms has been developed to facilitate the detection of surface cracks on bridge decks. By automating the crack detection process, this technology significantly improves the precision and effectiveness of maintenance activities.

Keywords : Highway bridges Simply Supported T-beam, Superstructure, internal force calculation, AutoCAD.

TABLE OF CONTENTS

摘要

| | |
|--|---|
| | |
| i | |
| ABSTRACT | |
| ii | |
| Chapter 1 Overview of Bridge | |
| Design..... | 1 |
| 1.1 Project Overview | |
| 1 | |
| 1.2 Design basis and main design | |
| specification..... | 1 |
| 1.3 Design technical | |
| standards..... | 2 |
| 1.4 Main Materials | |
| 2 | |
| 1.4.1SuperstructureMaterials | |
| 2 | |
| 1.5 Design Essentials | |
| 2 | |
| Chapter 2 Theoretical and Structural Design of Bridges | |
| 4 | |
| 2.1 | |
| Introduction..... | |

| | |
|---|----|
| | 4 |
| 2.2 Bridge Design Concepts | |
| | 5 |
| 2.2.1 Classification of Bridge | |
| | 5 |
| 2.2.2 Material Selection in the Bridge Construction..... | 6 |
| 2.3 Geological Condition | |
| | 7 |
| 2.4 Plan | |
| Comparison..... | |
| | 9 |
| Chapter 3 Calculation of the Reinforced Concrete T-Beam | |
| | 12 |
| 3.1 Design Data and Structural | |
| Layout..... | 12 |
| 3.1.1 Design | |
| Data..... | 1 |
| 2 | |
| 3.1.2 Design of Carriageway Slab | |
| | 13 |
| 3.1.3 Dead Load Internal Force | |
| | 14 |
| 3.1.4 Live load internal | |
| force..... | 14 |
| 3.1.5 Combination of internal force | |
| | 16 |
| 3.2 Reinforcement Design | |
| | 17 |
| 3.2.1 Reinforcement at fulcrum | |
| | 17 |
| 3.2.2 Reinforcement at Mid- | |
| span..... | 18 |
| 3.3 Calculation of connecting | |
| reinforcement..... | 20 |
| 3.3.1 Calculation effect of flexural member | |
| | 20 |
| Chapter 4. Design and Calculation of Main Beam | |
| | 23 |
| 4.1 Internal forces due to dead load are analyzsis | |
| | 24 |
| 4.2 Calculation of internal forces under live | |
| load..... | 26 |
| 4.3 Reinforcement design and strength checking calculation..... | 41 |
| 4.3.1 Principal longitudinal reinforcement arrangement | 41 |
| 4.3.2 Arrangement of shear reinforcement | |
| | 43 |
| 4.3.3 Main beam deflection verification calculation | 54 |
| Chapter 5 Calculations of | |
| Diaphragm..... | 56 |
| 5.1 Calculation of diaphragms | |
| | 56 |
| 5.2 Bending moment calculations of diaphragm | |
| | 58 |
| 5.3 Strength and reinforcement verification of diaphragm | 60 |
| 5.4 Shear force calculation and reinforcement design of the diaphragm..... | 63 |
| Chapter 6 Special Research | |
| | 66 |
| Transformation Medium-Span Bridge Design Through Advanced Materials and Digital | |
| Technologies for Sustainable Infrastructure | |
| | 66 |
| 6.1 Scientific Rationale and Innovative Context | |

| | |
|---|----|
| | 66 |
| 6.2 Innovative Materials in Medium Span Bridge Design | 67 |
| 6.2.1 Ultra High Performance Concrete (UHPC) | 67 |
| 6.2.2 Fibre Reinforced Polymers (FRP) | 67 |
| | 67 |
| 6.2.3 High-Strength Steel (HSS) | 68 |
| 6.3 Integration of Digital Technologies in Bridge Engineering | 69 |
| 6.3.1 Building Information Modelling (BIM) | 69 |
| 6.3.2 Digital Twin (DT) | 70 |
| | 70 |
| 6.3.3 Structural Health Monitoring (SHM) | 71 |
| 6.4 Case Study : Implementation in China | 72 |
| | 72 |
| 6.4.1 Project Xiamen Second East Passage | 72 |
| | 73 |
| 6.4.2 Hong Kong - Zhuhai - Macau Bridge (HZMB) | 73 |
| 6.5 Policy and Institutional Framework | 74 |
| 6.5.1 Harmonising international standards | 74 |
| | 75 |
| 6.5.2 Strengthening human resources capacity | 75 |
| 6.5.3 Investment in cross-cutting research | 75 |
| REFERENCE | 77 |
| AKNOWLEDGEMENT | 86 |

Chapter 1 Overview of Bridge Design

1.1 Project Overview

Liuquan Medium Bridge is a bridge project planned to be built at chainage point K52+335.500, is part of the Rongcheng-Wuhai Expressway (G18), commonly known as the Rongwu Expressway. The expressway connects the city of Rongcheng in Shandong Province with Wuhai City located in the Inner Mongolia Autonomous Region. In particular, this bridge is located on the road section between Xushui and Laiyuan in Hebei Province, which forms part of the fourth east-west corridor under the framework of the country's expressway development, commonly known as the "horizontal 18". The bridge alignment starts from the piling point of K52+311.550, reaches the midpoint at K52+335.500, and the end point at di K52+ 359.500. Bridge structure is designed to withstand the load according to the Type Highway Grade I, with the structural safety level set at Level I, the bridge deck clearance is 7m + 2 × 0.75m.

The bridge site lies on flat terrain, easing foundation work. Natural drainage occurs via surface runoff and evaporation, with seasonal water level changes. The non-corrosive surface water enhances concrete durability. Geotechnically, the site has fine clay with low bearing capacity, requiring ground improvement or deep foundations. Seismically, it falls under Design Category B, requiring resistance to moderate to strong earthquakes per national codes. The bridge must also meet Highway Grade I, supporting heavy commercial traffic and severing as a key of the part regional transport network.

1.2 Design basis and main design specification

1. (Ministry of Transport of the People's Republic of China, 2015). Specifications for the design of highway and culverts (in Chinese). Beijing: China Communications press.

2. (Ministry of Transport of the People's Republic of China, 2018). Code for the design of highway reinforced and prestressed concrete bridges and culverts (in Chinese). Beijing: China Communications Press.

3. (Jianguo, Yi, 2020). Bridge Calculation Example Series-Concrete Simply Supported Girder (Slab) Bridge. Beijing People's Traffic Press.

4. (AASHTO, 2012). Bridge design specifications based on load and resistance factor design (LRFD), units C.

5. (Highway Bridge and Culvert Design Manual - Girder Bridges (Upper Volume). press, People traffic, 1998).

6. Ye Mishu, edited by Ye Mishu (Mishu, 2020), 2020. Principles of Structural Design. Beijing : People's Transportation Press.

7. Yuan Lunyi and Bao Weigang, " (Weigang, 2004), Example of Application of Province. Beijing : People's

1.3 Design technical standards

1. Road Classification : The road is classified as a Highway Grade I structurally safe rated Level 1.
2. Bridge Deck Clearance : The clearance consists of 0.75 m sidewalk, 7.00 m clear lane and another 0.75 m sidewalk.
3. Lane Load Standard : The load standard lanes follow the specifications for Highway Class Grade I.
4. Design Slope : The maximum long slope is 2.5%, while the cross slope is 1.5%.
5. Seismic Protection Level : The seismic fortification is designed according to a seismic intensity of Level VII.

6. Compliance with Design Standards the route and other elements conform to the design regulations for highways.

1.4 Main Materials

1.4.1 Superstructure Materials

a) Concrete: The T-shaped main beams, heads and hinged joints of the bridge are made of Grade 30 concrete, and the bridge deck's cushion layer is made of C25 concrete. b) Reinforcing Steel: The main steel bars are HRB400 and the subsidiary reinforcement are HPB300. c) Expansion Joints: This type of product is a C30 series modular device produced by professional qualified manufacturers at the provincial or ministerial level.

1.5 Design Essentials

1. Bridge Layout : The bridge consists of eight girders combined with spans made of 21.50 m steel armatures on one level with a regular deck. The cross-section consists of five prefabricated T-beams made of reinforced concrete, placed at an interval of 1.6 m. Transverse slope is achieved via the sloping support beams and deck cover

2. Slope Adjustment on Deck Cover Beam : The cover beam can be tilted to adjust the transverse slope of the bridge deck.

3. Transverse Load Distribution Methodology : The coefficient for transverse load distribution at the structure's mid-span, affected by concentrated loads on the carriageway, is calculated using the eccentric pressure technique. For distributed loads and at the support regions, the coefficient is evaluated using the lever principle approach. Additionally, variations in the transverse distribution coefficient along the bridge span are taken into consideration during the vehicle load analysis.

4. Design of Main Beam : Load on each main beams comprises of the weight of safety barriers, fences etc uniformly distributed along the bridge superstructure. The reinforcement details are provided as per the common drawings.

5. Design of deck cover beam : The length of cover beam is calculated considering the worst negative vehicle loading arrangement. The reinforcement arrangement is as per the standard specifications.

6. Bridge Deck Reinforcement : In order to reduce cracking at the negative moment regions of the deck, reinforcement is directed toward the pavement layer above the pier caps.

7. Design Approach : While designing the bridge, use of Limit State method was ensured.

Chapter 2 Theoretical and Structural Design of Bridges

2.1 Introduction

The bridge plays a crucial role in the transport system in this modern era as a crucial element that enables connectivity between regions or cities to support the smooth movement of people and logistics distribution. The design of bridges not only focuses on an aspect of structural strength, but also must consider resistance to dynamic loads, extreme environmental influences, and the ability to respond to earthquakes. Due to the increasing emphasis on structure safety, Performance Based Seismic Design (PBSD) has become a fundamental strategy to guarantee bridges perform optimally during seismic events, particularly in earthquake-prone areas like China (Li et al., 2024).

An effective method of mitigating the impact of seismic events on bridge structures is to use seismic isolation, such as Friction Pendulum Bearing (FPB). This innovation helps regulate the inherent vibrations of the structure to achieve better dynamic performance, so that the earthquake force that reaches the bridge can be properly reduced. According to research conducted by Wang et al. (2021), the application of the FPB (Friction Pendulum Bearing) system in corrugated steel bridge structures has demonstrated a notable effectiveness in mitigating structural vibrations and dynamic impacts induced by seismic activities.

On another hand, advances in construction material technology have also contributed to the creation of a better and stronger bridge structure system. One such material that shows excellent performance referse to Ultra High Performance Concrete (UHPC). UHPC is widely used in precast joints due to its high strength and also its ability to withstand shock loads well. Xu et al. (2021) through an experimental study stated that precast connections using UHPC are able to behave like cast-in-place structures and provide resistance to cyclic loads without experiencing significant damage (Xu et al., 2021).

A further study conducted by Zhang et al. (2020) also reinforced the advantages of UHPC by applying a socket connection system equipped with shear keys to precast bridge columns. Experimental results state that

this method provides structural performance equivalent to conventional methods, and can even significantly reduce structural damage (Zhang et al., 2020).

The latest approaches in earthquake-resistant bridge design are starting to combine UHPC with smart materials such as Shape Memory Alloy (SMA). This material has the characteristic of self-centering after deformation, so it is effective in reducing residual deformation due to earthquakes. Li et al. (2024) stated that the application of a combination of UHPC and SMA in a bridge column can reduce residual deformation by almost 60% compared to conventional concrete columns, and provide better structural stability after an earthquake (Li et al., 2024).

All of these developments are also supported by advances in digital modelling technology in civil engineering, such as the use of the Finite Element Method (FEM). With this method, structural performance analysis, especially on UHPC joints, can be carried out accurately and efficiently. Zhang et al. (2020) stated that the results of numerical simulations are able to replicate experimental data precisely, which is very useful in optimising the design of earthquake-resistant bridge structures. Therefore, the integration of performance-based design approaches, earthquake isolation systems, material innovations such as UHPC and SMA, as well as the support of digital simulation technology are the main foundations in the development of bridge infrastructure that is adaptive to earthquake risks and has a longer service life.

2.2 Bridge Design Concepts

2.2.1 Classification of Bridge

Bridges can be classified based on the basic components & category of the bridge:

- 1) By the size of the bridge : Super major bridge, major bridge, medium bridge, small bridge, culvert, etc.
- 2) By usage : Highway bridge, railway bridge, rail road bridge, foot bridge, pipeline bridge, water bridge or aqueduct, etc.
- 3) By type of construction material: such as flexural concrete structures reinforced with steel bars, tensioned concrete spans with pre-applied stress, metallic frameworks primarily composed of steel, hybrid structure combining multiple materials, wooden beam crossings, and other variants built from unconventional or blended substances.
- 4) By location of the bridge deck: Types include the above deck type, through type, and half through type.
- 5) By horizontal curve : Straight bridge, skew bridge, and curved bridge.
- 6) By expected service time : Permanent bridge and temporary bridge.
- 7) By the obstacle crossed through : River crossing bridge, sea crossing bridge, overpass bridge, and viaduct.

8) By mobility of the bridge : Fixed bridge, moveable bridge include bascule bridge, lift bridge, swing bridge and floating bridge.

9) By structure system : Beam bridge, arch bridge, suspension bridge, combination system bridge, etc. In addition to the classification of bridges, according to research by Jooto and Lattanzi (2018), how to calculate the type of bridge structure is done with a learning approach using data from the National Bridge Inventory (NBI) on U.S. territory. The dataset comprises over 600.000 bridges, each with a variety of key technical parameters, allowing classification into 23 distinct structural categories. Of these, there are 4 main types that are most commonly used in the United States, namely:

1) Stringer/Multi Beam or Girder Bridges

This bridge is the most dominant structural type, accounting for about 41% of all bridges listed. The most dominant characteristic is the use of longitudinal beams as the main support element for the bridge deck.

2) Covert (Culvert) Bridges

With about 23% of the total bridge population. This type of bridge is generally used on small watercourses or as a water channel under the road.

3) Slab Bridge

This plate bridge covers about 14% of the total data and is generally used for short spans. The bridge deck serves as the main structural element without additional beams.

Besides these four main types, other classifications recorded in the database include truss, arch, and other combinations of structural systems. Each of these structural types was selected based on technical considerations such as span length, traffic load, geotechnical conditions, and the level of seismic activity at the construction site.

2.2.2 Material Selection in the Bridge Construction

The selection of materials in bridge construction is a crucial factor that determines structural strength, environmental resistance, service life, and construction cost efficiency. Therefore, material selection must consider mechanical properties, corrosion resistance, and environmental sustainability aspects.

1) The load capacity and durability of high strength steel

High-strength steel has become the first choice in bridge construction due to its ability to optimally support static and dynamic loads. According to research conducted by Wang et al. (2021), this type of steel is not only superior in terms of mechanical strength, but also has high resistance to corrosion when given appropriate protective treatment. The research states that anti-corrosion coating techniques and specialised

strengthening methods can extend the steels resistance to damage from exposure to extreme environments, such as coastal climatic conditions rich in chloride ions.

By utilizing high-strength steel, bridges can be built with extended spans and reduced structural weight, which leads to improved material efficiency and lower maintenance expenses over time. Therefore, it is highly recommended for applications in bridges that require high structural performance and optimal environmental resistance.

2) The environmental resilience and use of fly ash in concrete

Using fly ash as the main ingredient in concrete mixtures is one of the solutions to improve durability and sustainability aspects in bridge construction. Based on the study by Zhang et al. (2020), incorporating fly ash enhances the physical and chemical characteristics of concrete, thereby increasing its resistance to chloride ion penetration, which may result in the degradation of the reinforcing steel through corrosion.

| | | |
|--|--|--|
| 指 标 | | |
| 疑似剽窃文字表述 | | |
| <div>1. seismic fortification is designed according to a seismic intensity of Level VII.</div> <div>6.Compliance with Design Standards the route and other elements conform to the design regulations for highways.</div> <div>1.4Main Materials</div> <div>1.4.1Superstructure Materials</div> <div>a) Concrete: The T-shaped main beams, heads and hinged joints of the bridge</div> | | |
| 2. Scheme design and calculation of Liuquan Medium bridge on Rongwu highway_第2部分 | | 总字数: 16096 |
| 相似文献列表 | | |
| 去除本人文献复制比: 4.9%(788) 去除引用文献复制比: 4.9%(788) 文字复制比: 4.9%(788) 疑似剽窃观点: (0) | | |
| 1 | Scheme Design and Structural Calculation of Chayuan middle-span bridge on Rongwu Highway NAURA BERLIAN HUMAIROH - 《大学生论文联合比对库》 - 2024-06-14 | <div>4.9% (788)</div> <div>是否引证: 否</div> |
| 原文内容 | | |

Within the scope of the study, it is stated that concrete mixed with fly ash has fewer pores and a denser microstructure than ordinary concrete. These conditions can slow down the penetration of harmful ions and delay the corrosion process of the reinforcement, thus increasing the life of the concrete. Moreover, incorporating fly ash contributes positively to environmental sustainability by decreasing the reliance on Portland cement, which in turn can lower carbon emissions associated with concrete manufacturing. So fly ash also plays a role in increasing the resistance of concrete to environmental factors, but also supports the principle of sustainable development in the field of bridge construction.

2.3 Geological Condition

According to the 2019 JTG 3363 guideline, geotechnical investigations must be conducted with a series of laboratory and field tests to generate data on the physical and mechanical characteristics of soils and rocks. The results of these tests are used in the evaluation of soil bearing capacity, prediction of settlement, and slope stability, which form the basis of foundation planning.

According to research conducted by Yin et al. (2022) stated that the slope of the land has a direct influence on the horizontal resistance coefficient value of the foundation, which has implications for structural stability. Therefore, under certain geographical conditions, an in-depth evaluation of the land contour is very important. The use of numerical models and three-dimensional geotechnical simulations is necessary to assess the interaction between geological conditions and structural response to dynamic and static loads.

In addition, according to research conducted by Zhu, Qian & Cai (2024), the calculation of horizontal displacement in soil retaining structures around foundation excavations is a crucial aspect, especially in urban environments or sites with limited working space. This research provides a relevant calculation approach in controlling lateral deformations arising from deep foundation work. Therefore, combining geological investigations with geotechnical engineering techniques is essential to guarantee the durability and long-term functionality of bridge foundations.

2.3.1 Classification of foundations based on JTG 3363 - 2019 standard

According to the guidelines set forth in JTG3363-2019, bridge foundation system are classified three

primary categories determined by their depth and method of load transfer, specifically :

1) Shallow Foundation

These foundation types, such as footings and raft foundations, are designed for use in surface soil conditions that have high bearing capacity. The load of the structure is spread evenly over a large area of soil, making it a technically and economically efficient solution for short to medium span bridges. According to the JTG standard, an analysis of both the total settlement and the soil's bearing capacity is necessary to verify that the foundation remains within acceptable serviceability and strength limits.

2) Deep Foundation

If the upper soil layer is unable to support the bridge load directly, a deep foundation system such as piles or bored piles is required. This system transfers the load to deeper and more stable soil or rock layers. In its use, it is necessary to evaluate the axial and lateral loads, as well as the combination between the two. In addition, JTG 3363-2019 requires consideration of special effects such as negative friction, lateral displacement of soil, and earthquake effects on the vertical components of the foundation.

3) Combination Foundations

For heterogeneous soil conditions or for structures with large weights, combinative approaches are often applied. One form of this is pile-reinforced raft foundations, which serve to reduce the risk of uneven settlement while increasing the overall bearing capacity of the system. In aquatic environments, structures such as caissons are used to build foundations below the water surface. The interaction between the foundation and the superstructure is also an important concern in design, as stipulated in these standards.

2.4 Plan Comparison

In the Liuquan Medium Bridge on Rongwu Highway, the plan comparison can be found in table 2.1.

Table 2. 1 Comparative analysis of scheme hierarchies

Scheme 1

Scheme 2

Scheme 3

Compare Reinforced Concrete Reinforced Concrete

Schemes

content

Simple-Support T- Continuous Beam

Arch Bridge

Beam Bridge

Bridge

The scheme reflects a Designed to enhance These bridge straightforward and structural performance structures utilise a cost-efficient

and load distribution, curved geometry

construction methods, this bridge type

configuration to

ideal for relatively

utilizes continuous

channel the

short spans. The

beams extending over dominant load in

structural designs uses multiple piers. The

the form of

individual T-shaped continuity reduces compressive forces

beams, each supported bending stress and towards the end

at its ends, allowing maximizes material supports. This

for simplified

usage, while also concept results in

1 Characteristics

execution, less

improving rigidity and high efficiency in

material consumption, reducing deflections. load-bearing,

and a shorter

However, it requires

especially at

construction

more detailed

medium to long

timeframe. Despite

planning, complex spans, having the
these advantages, its reinforcement layouts, advantage of
ability to handle
and typically takes
maintaining
longer spans is limited longer to build with structural stability
due to potential
higher associated
with minimal
deflection issues
costs.
deformation. This
under heavy loads.
type is commonly

2

3

used in conditions
that require large
bearing capacity
and long-term
performance.

This conventional Building on the T- The implementation
designs stands out for beam concept, this
of this type is

its ease of execution model introduces determined by the
and budget friendly continuous support readiness of basic
nature. It is most
across spans,
infrastructure such
effective for projects
improving the

as foundations and
with shorter lengths, bridge' s capacity to terrain conditions.
where quick assembly handle greater loads The construction
and minimal materials with less deformation. process requires
It is generally gradual stages with
are key

considerations. Eac

beam acts as an

h preferred for mid to greater technical
long spans projects. precision than other

Implementation independent unit,

performance

which simplifies

maintenance and

The tradeoff,

types, although the

however, lies in the processing time is

complexity of

relatively longer

calculations, detailing, and more resources

construction. That

said, the structure m

be more prone to

ay and construction are needed, but the

processes, all of which final result is a

deflection under

heavier loads, and

may increase overall stable and durable

project time and cost. structure so that this

lacks the structura

integration seen in
1
type is the main
consideration in its
selection, especially
more advanced
designs
in large-scale
infrastructure
projects.

Requirements reinforcing steel

Material

While the volume of Though this option is The materials used
more economical than in this system tend required is relatively the third schemes into be more complex.
low, the construction terms of cost and port Reinforced concrete
process particularly in handling, it involves
and steel are the
situ concrete castings
far more manual
main materials, and
is more labor
labor, a longer
during the
intensive. During the construction schedule,
construction
building phase, certain and large quantities of process, scaffolding
structural elements
masonry material
or temporary
must independently
support systems are
carry the load of the
required until all
freshly poured deck
elements work
concrete
together. Even
though the material
consumption is
greater than the
simple bridge type,
this type produces a
structure with high
durability and good
durability.

According to a thorough evaluation of various structural alternatives, including arch and suspension bridges, it was found that a simple reinforced concrete T-girder bridge scheme was the appropriate choice for this project. This is based on technical and economic considerations that are in accordance with the field conditions and functional needs of the bridge.

The simple T-girder structure offers ease of implementation, accelerated construction time, material efficiency, and is suitable for the 21.5 m span. It can also withstand class I traffic loads without excessive deflection and requires less reinforcement than the continuous or suspended types, making it more cost-effective and easier to supervise. In terms of maintenance, this system is also superior as each girder is independent, allowing for localised repairs without disrupting the entire structure.

In the calculations that have been carried out in the chapter below, it is stated that this scheme has fulfilled the applicable bridge design requirements. Therefore, scheme 1 was selected as the optimal final design based on resource efficiency, technical suitability, and ease of implementation.

Chapter 3 Calculation of the Reinforced Concrete T-Beam

3.1 Design Data and Structural Layout

3.1.1 Design Data

A. Main Beam

The main structure uses precast T-beams of reinforced concrete with a simply supported system and a standard span length of 21.50 m. The beam has a height of 155 cm, installed with an inter-beam spacing of 160 cm. The main beams are reinforced with five transverse diaphragms that serve as stabilising elements. The width of the beam ribs is 20 cm. At the bottom of the wing (flange root), it is up to 20 cm thick and thins gradually to 12 cm at the end. This dimension is built to support heavy traffic loads and ensure sufficient space width for two-way vehicle movement with multiple lanes.

Figure 3.1 Cross section and Longitudinal Section

1) Bridge Deck Clearance : 7m + 2 × 0.75m sidewalk

2) Span and Total Length of Main Beam

Calculated Span: = 21.50 m Total Length of Bridge: L = 22 m

3) Design Load

Highway Grade I a. Live load:

Highway Grade I, as prescribed by JTG D60-2015

Pedestrian uniform load: 3kN/m² b. Dead load:

Pavement: 2cm asphalt concrete layer (g=23kN/m³) and C25 concrete cushion

(g=24kN/m³). Flange plates of T-beams (g=25kN/m³).

4) Materials

Reinforcement: HRB400 reinforcement is used for main reinforcement.

Steel properties according to the table 3.1.1 :

Table 3. 1.1 Analytical specification for steel reinforcement bars

Design Modulus of Design tensile Standard Species compressive elasticity strength strength strength

HPB300(MPa) 2.1×10⁵ 250 250 300 HRB400(MPa) 2.1×10⁵ 330 330 400

B. The technical indicators of concrete

The technical indicators of are shown in the table 3.2.2 :

Table 3. 2.2 Concrete technical indicators

Design strength (MPa) Standard strength (MPa) Axial Axial Axial Axial Elastic modulus Species Crushing

Tension Tension Tension (MPa) Strength Strength Strength Strength C25 11.9 1.27 16.7 1.78 2.80 104 C30 14.3 1.43 20.1 2.01 3.00 104

3.1.2 Design of Carriageway Slab

Monodirectional slab :

Clear span : $l_0 = 160 - 20 = 140 \text{ cm} = 1.40 \text{ m}$

Thickness of deck : $t = 12 + 20 = 16 \text{ cm} = 0.16 \text{ m}$

Calculation bending moment : $l = l_0 + t = 140 + 16 = 156 \text{ cm} = 1.56 \text{ m}$

Calculation shear force : $l = l_0 = 140 = 1.40 \text{ m}$

Impact factor is $1 + \mu = 1.3$

3.1.3 Dead Load Internal Force

Pavement: 2 cm asphalt concrete layer ($g = 23 \text{ kN/m}^3$), C25 concrete cushion ($g = 24 \text{ kN/m}^3$), and flange plates of T-beams ($g = 25 \text{ kN/m}^3$).

The longitudinal 1.0, is wide strip is taken for calculation :

Table 3. 3.3 Dead load internal force

Asphalt concrete surface (g₁)

$0.02 \text{ m} \times 1.0 \text{ m} \times 23 \text{ kN/m}^3 = 0.46 \text{ kN/m}$

C25 concrete cushion (g₂)

$0.12 \text{ m} \times 1.0 \text{ m} \times 24 \text{ kN/m}^3 = 2.88 \text{ kN/m}$

$0.12 \text{ m} +$

(g₃)

2

Dead weight of T-beam flange

0.20 m

$\times 1.0 \text{ m} \times 25 \text{ kN/m}^3 = 4.00 \text{ kN/m}$

Total

3

$g = \sum_{i=1} g_i = 7.34 \text{ kN/m}$

i-1

The moment caused by the dead load at the structure's midpoint is a critical factor that must be considered during the planning phase :

$M_{og} = g l^2 / 8 = 7.34 \times 1.56^2 / 8 = 2.23 \text{ kN} \cdot \text{m}$ $Q_{og} = g l / 2 = 7.34 \times 1.40 = 5.14 \text{ kN}$

3.1.4 Live load internal force

A. Calculation the effective distribution width

The length of a rear wheel landing of a vehicle load is $a_2 = 0.20$ m has a width of $b_2 = 0.60$ m.

1) Thickness of pavement

$H = \text{asphalt concrete pavement} + \text{concrete cushion}$

$$= 2 \text{ mm} + 12 \text{ mm} = 14 \text{ mm} = 0.14 \text{ m}$$

2) The distributing rectangle of the load is with the size of :

$$a_1 = a_2 + 2H = 0.20 + 2 \times 0.14 = 0.48 \text{ m} \quad b_1 = b_2 + 2H = 0.60 + 2 \times 0.14 = 0.88 \text{ m}$$

For a single load $l = 1.56$ m, so we used :

$$l \quad a = a_1 + 3 \quad 1.56 \quad 2 \quad 2 \quad a = 0.48 + = 1 < (\times 1 = \times 1.56 = 1.04 \text{ m}) \quad 3 \quad 3 \quad a' = a_1 + t \quad 1 \quad 1.56 \quad a' = 0.48 + 0.16 = 0.64 > (= = 0.52 \text{ m}) \quad 3 \quad 3 \quad a' = 0.64 \text{ m} \quad a_x = a' + 2x \quad a_x = 0.64 + 2x$$

3) Live load bending moment

$$P \quad b_1 \quad M_{op} = (1 + \mu) \times (1 -) \quad 8a \quad 2 \quad 140 \quad 0.88 \quad M_{op} = (1 + 0.3) \times (1.56 -) = 24.50 \text{ kN} \cdot \text{m} \quad (8 \times 1.04) \quad 2$$

4) Shear calculation of live load $l = 10 = 1.40$ m

•The load located in the center area :

$$l \quad 1.40 \quad 2 \quad 2 \quad a = a_1 + = 0.48 + = 0.95 \leq (l = \times 1.40 = 0.93 \text{ m}) \quad 3 \quad 3 \quad 3 \quad 3$$

No overlap and then we can get, $a = 0.95$ m

• The load located on the support :

$$l \quad 1.40 \quad a' = a_1 + t = 0.48 + 0.16 = 0.64 \text{ m} \geq (= = 0.47 \text{ m}) \quad 3 \quad 3$$

No overlap then we can get, $a' = 0.64$ m

$$a - a' \quad 0.95 - 0.64 = = 0.155 \text{ m} \quad 2 \quad 2 \quad P \quad 140 \quad A_1 = = = 73.68 \quad 2a \quad (2 \times 0.95) \quad P_2 \quad A_2 = (a - a') \quad 8aa' \quad b_1 \quad 140 = (0.95 - 0.64)^2 = 3.14 \quad (8 \times 0.95 \times 0.64 \times 0.88) \quad 0.88 \quad 1.40 - (2) \quad y_1 = = 0.69 \quad 1.40$$

$$l \quad 1.40 - 3 \times 0.155 \quad y_2 = = 0.96 \quad 1.40$$

Figure 3. 2 Deck composition

$$Q_{op} = (1 + \mu) (A_1 y_1 + A_2 y_2) = (1 + 0.3) ((73.68 \times 0.69) + (3.14 \times 0.96)) = 70.01 \text{ kN}$$

3.1.5 Combination of internal force

1) Internal force combination in limit State of bearing capacity

$$M_{ud} = 1.2M_{og} + 1.8M_{op} = 1.2 \times 2.23 + 1.8 \times 24.50 = 46.78 \text{ kN} \cdot \text{m} \quad Q_{ud} = 1.2Q_{og} + 1.8Q_{op} = 1.2 \times 5.14 + 1.8 \times 70.01 = 132.19 \text{ kN} \quad 12 + 20 \text{ h} = 155 - = 139 \text{ cm} = 1.39 \text{ m} \quad 2 \quad t \quad 0.16 = = 0.12 \leq 0.25 \text{ h} \quad 1.39$$

So we can get :

$$M_{mid} = +0.5M_{ud} = 0.5 \times 46.78 = 23.39 \text{ kN} \cdot \text{m}$$

$$M_{fc} = -0.7M_{ud} = -0.7 \times 46.78 = -32.75 \text{ kN} \cdot \text{m}$$

2) Internal force combination in normal service limit state

A. Short term effect combination

$$24.5 \quad M_{fd} = M_{og} + 0.7M_{op} = 2.23 + 0.7 () = 15.42 \text{ kN} \cdot \text{m} \quad 1.3 \quad 70.01 \quad Q_{fd} = Q_{og} + 0.7Q_{op} = 5.14 + 0.7 () = 42.84 \text{ kN} \quad 1.3 \quad \text{So we can get : } M_{mid} = +0.5M_{ud} = 0.5 \times 15.42 = 7.71 \text{ kN} \cdot \text{m} \quad M_{fc} = -0.7M_{ud} = -0.7 \times 15.42 = -10.79 \text{ kN} \cdot \text{m}$$

B. Long term effect combination

$$24.5 \quad M_{fd} = M_{og} + 0.4M_{op} = 2.23 + 0.4 () = 9.77 \text{ kN} \cdot \text{m} \quad 1.3 \quad 70.01 \quad Q_{fd} = Q_{og} + 0.4Q_{op} = 5.14 + 0.4 () = 26.68 \text{ kN} \quad 1.3 \quad \text{So we can get : } M_{mid} = +0.5M_{ud} = 0.5 \times 9.77 = 4.89 \text{ kN} \cdot \text{m} \quad M_{fc} = -0.7M_{ud} = -0.7 \times 46.78 = -6.84 \text{ kN} \cdot \text{m}$$

3.2 Reinforcement Design

In this design we adopts the 1 m wide strip for reinforcement calculation.

3.2.1 Reinforcement at fulcrum

C25 Concrete and HRB400, from the table :

Table 3.2. 1 Reinforcement at Fulcrum

$$\begin{array}{cccccc} \text{fck(Mpa)} & \text{ftk(Mpa)} & \text{fcd(Mpa)} & \text{ftd(Mpa)} & \text{Ec(Mpa)} & \text{C25} \end{array} \quad \begin{array}{cccccc} 16.7 & 1.78 & 11.5 & 1.23 & 2.80 \times 10^4 & \text{C30} \end{array} \quad \begin{array}{cccccc} 20.1 & 2.01 & 13.8 & 1.39 & 3.00 \times 10^4 \end{array}$$

According to the information in the table 3.2.1 , we can conclude that :

$$f_{cd} = 11.5 \text{ Mpa}; f_{td} = 1.23 \text{ Mpa}; f_{sd} = 330 \text{ Mpa}; \epsilon_b = 0.58.$$

The structure is covered by a 20 mm thick protective layer, with an effective of $h_0 = 155 - 20 = 135$ mm, $M_d = -32.75 \text{ kN} \cdot \text{m}$. This equation adheres to the requirements set forth in Article 5.2.2 relating to the standardized guidelines for the structural design of reinforced concrete highways alongside highway bridge concrete culvert structures.

$$a \quad \gamma_0 M_d \leq f_{cd} b a (h_0 -) \quad 2 \quad a \quad 1.1 \times 32.75 \leq 11.5 \times 10^3 \times 1.0 a (0.135 -) \quad 2 \quad a \quad 36.025 \leq 11500 \times a (0.135 -) \quad 2 \quad 36.025 \leq a (0.135 - 0.5a) \quad 11500 \quad 0.5a^2 - 0.135a + 0.003 \leq 0 \quad a \approx 0.025 \text{ or } x \approx 0.025$$

$$\text{and then check } \epsilon_b h_0 = 0.58 \times 0.135 = 0.079 \text{ m} \geq x = 0.025 \text{ m}$$

$$f_{sd} A_s = f_{cd} b' f x \quad 11.5 \times 1.0 \times 0.025 \quad A_s = 330 \quad A_s = 8.71 \text{ cm}^2$$

Inspection of the Reinforcement cross-section table 3.2.2 with a spacing of 1 m from the width of the plate, reinforcement $\phi = 12$ with a spacing of 125 mm, then the cross-sectional area of the bone used :

| | | | |
|---|---|--|-------------------------|
| 指 标 | | | |
| 疑似剽窃文字表述 | | | |
| <div>1. = 70.01 kN</div> <div>3.1.5 Combination of internal force</div> <div>1) Internal force combination in limit State of bearing capacity</div> <div>Mud = 1.2Mog + 1.8Mop = 1.2 × 2.23 + 1.8 ×</div> <div>2. 5 kN • m</div> <div>2) Internal force combination in normal service limit state</div> <div>A. Short term effect combination</div> <div>24.5 Mfd = Mog + 0.7Mop =</div> <div>3. 6.84 kN • m</div> <div>3.2Reinforcement Design</div> <div>In this design we adopts the 1 m wide strip for reinforcement calculation.</div> <div>3.2.1Reinforcement at fulcrum</div> <div>C25 C</div> | | | |
| 3. Scheme design and calculation of Liuquan Medium bridge on Rongwu highway_第3部分 | | | 总字数: 16709 |
| 相似文献列表 | | | |
| 去除本人文献复制比: 14.2%(2365) 去除引用文献复制比: 14.2%(2365) 文字复制比: 14.2%(2365) 疑似剽窃观点: (0) | | | |
| 1 | Scheme design and calculation of Xiaoxin River Middle-span bridge on Rongwu highway | YERIBU PROSPER AWOLEBA - 《大学生论文联合比对库》 - 2024-07-02 | 13.8% (2306) 是否引证: 否 |
| 2 | 地铁站侧墙混凝土温度应力及裂缝防治研究 | 周集权(导师: 王晓睿) - 《华北水利水电大学硕士学位论文》 - 2023-06-01 | 0.4% (59) 是否引证: 否 |
| 原文内容 | | | |

$A_g = 9.05 \text{ cm}^2 \geq 8.71 \text{ cm}^2$
And the size of the bending members with a leaving cross-section shall meet the requirements of :
 $\rho = 905 = 0.670\% \geq \rho_{\text{min}} (0.45 f_{ft} / f_y) = \rho_{\text{max}} (0.45 f_{td} / f_y) = 0.34\% 1000 \times 135 \text{ sd min}$
So the requirement is met.
3.2.2 Reinforcement at Mid-span
The effective height $h_0 = 155 - 20 = 135 \text{ mm}$, $M_d = 23.39 \text{ kN} \cdot \text{m}$
 $a \gamma_0 M_d \leq f_{cd} b a (h_0 -)^2 a 1.1 \times 23.39 \leq 11.5 \times 10^3 \times 1.0 a (0.135 -)^2 a 25.729 \leq 11500 a (0.135 -)$
2 5.750a² - 1552.5a + 25.729 ≤ 0 a ≈ 0.0177 or x = 0.0177
and then check $\epsilon_{bh0} = 0.58 \times 0.135 = 0.079 \text{ m} \geq x = 0.0177 \text{ m}$
 $f_{sd} A_s = f_{cd} b' f_x$
 $11.5 \times 1.0 \times 0.0177 A_s = 330$
 $A_s = 6.133 \text{ cm}^2$
Table 3.2. 2 Rebar cross-sectional are per meter width (fixed spacing)
Rebar Spacing
Rebar Diameter (mm)
(Mm)
6 8 10 12 14 16 18 20 22 24
70
404 718 1122 1616 2199 2873 3636 4487 5430 6463
75
377 670 1047 1508 2052 2681 3393 4188 5081 6032
80
353 628 982 1414 1924 2514 3181 3926 4751 5655
85
333 591 924 1331 1811 2366 2994 3695 4472 5322
90
314 559 873 1257 1711 2234 2828 3490 4223 5027

95
 298 529 827 1190 1620 2117 2679 3306 4001 4762
 100
 283 503 785 1131 1539 2011 2545 3141 3801 4524
 105
 269 479 748 1077 1466 1915 2424 2991 3620 4309
 110
 257 457 714 1028 1399 1828 2314 2855 3455 4113
 115
 246 437 683 984 1339 1749 2213 2731 3305 3934
 120
 236 419 654 942 1283 1676 2121 2617 3167 3770
 125
 226 402 628 905 1232 1609 2036 2513 3041 3619
 130
 217 387 604 870 1184 1547 1958 2416 2924 3480
 135
 209 372 582 838 1140 1490 1885 2327 2816 3351
 140
 202 359 561 808 1100 1436 1818 2244 2715 3231
 145
 195 347 542 780 1062 1387 1755 2166 2621 3120
 150
 189 335 524 754 1026 1341 1697 2084 2534 3016
 155
 182 324 507 730 993 1297 1642 2027 2452 2919
 160
 177 314 491 707 962 1257 1590 1964 2376 2828
 165
 171 305 476 685 933 1219 1542 1904 2304 2741

Inspection of the Reinforcement cross-section table 3.2.2 with a spacing of 1 m from the width of the plate, reinforcement $\phi = 10$ with a spacing of 125 mm, determine the cross-sectional area of the bone used :

$$A_g = 6.28 \text{ cm}^2 \geq 6.133 \text{ cm}^2$$

And the size of the bending members with a leaving cross-section shall meet the requirements of :

$$\rho = 628 = 0.47\% \geq \rho_{\min} \text{ (0.45 ff td 0.2\%)} = \rho_{\max} (0.45 \text{ 13.3203 } 0.2\%) = 0.34\% \text{ 1000 } \times 135 \text{ sd min}$$

So the requirement is met.

$$(0.51 \times 10^{-3}) \sqrt{f_{cu}} k b h_0 (0.51 \times 10^{-3} \sqrt{25} \times 1000 \times 135 = 344.25 \text{ kN} \geq Q_{ud} = 132.19 \text{ kN}$$

$$(0.625 \times 10^{-3}) a_2 f_t d b h_0 (0.625 \times 10^{-3}) \times 1 \times 1.23 \times 1000 \times 135 = 103.78 \text{ kN}$$

Therefore, the evaluation of the shear strength for the sloped segment is deemed unnecessary, it is sufficient to design the stirrups according to structural specifications. Therefore, the following calculation of bearing capacity is checked:

$$f_s d A_s x = f_{cd} b' f 330 \times 0.0006133 x = 0.0176 \text{ 11.5 } \times 1.0 \times M_d = f_{cd} b' f x (h_0 -) 2 0.0176 M_d = 11.5 \times 103 \times 1.0 \times 0.0176 \times (0.135 -) = 25.54 \text{ kN} \cdot \text{m} \quad M_d = 25.54 \text{ kN} \cdot \text{m} \geq 23.39 \text{ kN} \cdot \text{m} \quad \text{The requirement is met.}$$

3.3 Calculation of connecting reinforcement

3.3.1 Calculation effect of flexural member

$$P_{12} q_{13} \omega_{BP} = \eta (1 + \mu) - \eta (1 + \mu) 16EI 24EI$$

Where :

μ I_b R_b E_b : Transverse distribution coefficient of main beam load ($\eta = 0.681$) : Impact coefficient, $(1 + \mu) = 1.3$ η : Converted inertia moment of main beam ($I_b = 11.43 \times 10^{-2} \text{ m}^4$) : Bearing reaction under live load
 1 : Modulus of elasticity of main beam ($E_b = 2.8 \times 10^4 \text{ Mpa}$) $h_s = 4.2 \text{ cm}$ $A_s = 36 \text{ cm}^2$ $E_s = 4.6 \times 10^2 \text{ Mpa}$:

Length of connecting rod ($l = 90 \text{ cm}$)

α : Distance between two supports ($\alpha = 50 \text{ cm}$)

After that substitution the corner and vertical displacement on the left side have been corrected :

Characteristic magnitude of the evenly spread load :

$$q_k = 10.5 \text{ kN/m}$$

So :

$$q_{13} \omega_{BP} = - \eta (1 + \mu) 24EI 10.5 \times 21.53 \omega_{BP} = -0.681 \times 1.3 \times 24 \times 2.8 \times 10^4 \times 0.1143 \times 1000 \omega_{BP} = -12.03 \times 10^{-4} = -1.203 \times 10^{-3} \text{ q1 RBP} = \eta (1 + \mu) 16EI 10.5 \times 21.5 \text{ RB} = 0.681 \times 1.3 \times = 99.93 \text{ kN } 2 0.042 \times 99.93 0.9 - 0.5 \Delta B = - \times (-12.03 \times 10^{-4}) 0.036 \times 4.6 \times 10^5 2 \Delta B = (2.54 \times 10^{-4}) - (-2.406 \times 10^{-4}) \Delta B = 4.856 \times 10^{-4} = 0.4856 \times 10^{-3}$$

The corner and vertical displacement at the left is obtained as follows:

$$P12 \quad \omega'_{AP} = \omega_{BP} - \eta(1 + \mu)16EI \quad 299 \times 21.52 \quad \omega'_{AP} = -12.03 \times 10^{-4} - 0.681 \times 1.3 \times 16 \times 2.8 \times 104 \times 0.1143 \times 1000 \quad \omega_{AP} = -3.59 \times 10^{-3} \quad q1 \quad R'_{A} = \eta(1 + \mu)16EI \quad 10.5 \times 21.5 + 299 \quad R'_{A} = 0.681 \times 1.3 \times = 232.28 \text{ kN} \quad 2 \quad 0.042 \times 232.28 \quad 0.9 - 0.5 \quad \Delta'_{A} = - \times (2.51 \times 10^{-3}) = 0.871 \times 10^{-3} \quad 0.036 \times 4.6 \times 105 \quad 2$$

Then, calculation of fixed end bending moment connection rod :

$$E cIc \quad 6 \Delta b \quad 6 \Delta A \quad MB = (- 4 \omega_{BP} + 2 \omega'_{AP} -) \quad 11 \quad 1 \quad EcIc \quad 6 \times 0.4856 \times 10^{-3} \quad 6 \times 0.871 \times 10^{-3} \quad MB = (- (4 \times (1.203 \times 10^{-3}) - (2 \times 3.59 \times 10^{-3}) - ())) \quad 0.90 \quad 0.90 \quad 0.90$$

$$EcIc \quad MB = (-14.56 \times 10^{-3}) = -16.17 \times 10^{-3} EcIc \text{ kN} \cdot m \quad 0.90 \quad EcIc \quad 6 \Delta'_{A} \quad 6 \Delta B \quad M'_{A} = (+ 2 \omega_{BP} + 4 \omega'_{AP} -) \quad 11 \quad 1 \quad Ec \quad Ic \quad 6 \times 0.871 \times 10^{-3} \quad 6 \times 0.4856 \times 10^{-3} \quad M'_{A} = (+ (2 \times (1.203 \times 10^{-3}) + (4 \times 3.59 \times 10^{-3}) + ())) \quad 0.90 \quad 0.90 \quad 0.90 \quad E cIc \quad Mb = (25.81 \times 10^{-3}) = 28.68 \times 10^{-3} EcIc \text{ kN} \cdot m \quad 0.90$$

The following is the calculation of reinforcement stress, with the HRB400 and $\phi 20$:

$$My \quad d \quad 2 \quad \sigma_A = , \quad \text{take } y = = 1.0 \text{ cm}, \quad M = M'_{A}, \text{ so } : \quad Ic \quad 2 \quad 28.68 \times 2 \times 103 \times 103 \times 10^{-3} \times Ic \times 0.01 \quad \sigma_A = = 57.36 \text{ Mpa} \quad Ic$$

Therefore :

$$\sigma_A = 57.36 \ll \sigma_s = 195 \text{ Mpa}$$

Chapter 4. Design and Calculation of Main Beam

This main beam was designed using C30 Concrete, which was selected for its high strength and reliable durability, with $E_c = 3.00 \times 10^4$, $f_{ck} = 20.1 \text{ Mpa}$, $f_{cd} = 13.8 \text{ Mpa}$, $f_{tk} = 2.01 \text{ Mpa}$, $f_{td} = 1.39 \text{ Mpa}$. The parameters are important to ensure structural integrity under both compression and tension.

HRB400 steel reinforcement is also used as ordinary reinforcement, which has a design tensile strength of $f_{sd} = 330 \text{ Mpa}$. The overall cross-section size of the monolith beam is established by structural needs, the full details of which are given in following sections:

Table 4. 1 Standard and design concrete strength values (MPa)

符

混凝土抗压强度等级

强度种类

号C25C30C35C40C45C50C55C60C65C70C75 C80

强度轴心抗

fck

压强度

16. 720. 123. 426. 829. 632. 435. 538. 541. 544. 547. 4 50. 2

标准

值

轴心抗

ftk1. 782. 012. 202. 402. 512. 652. 742. 852. 933. 03. 05 3. 10

拉强度

强度设

轴

压

心

强度

抗

fcd11. 513. 816. 118. 420. 522. 424. 426. 528. 530. 532. 4 34. 6

计值轴心抗

ftd1. 231. 391. 521. 651. 741. 831. 891. 962. 022. 072. 20 2. 14

拉强度

Table 4. 2 Modulus of elasticity of concrete ($\times 10^4 \text{ Mpa}$)

混凝土抗压强度等级 C25 C30 C35 C40 C45 C50 C55 C60 C65 C70 C75 C80

Ec

2. 80 3. 00 3. 15 3. 25 3. 35 3. 45 3. 55 3. 60 3. 65 3. 70 3. 75 3. 80

Figure 4. 1 T-beam cross sectional size of the main beam (cm)

4.1 Internal forces due to dead load are analyzsis

1) Self-weight on main beam

$$0.12 + 0.20 \quad g1 = \{ (0.20 \times 1.55) + () (1.16 - 0.20) \} \times 25 = 13.35 \text{ kN/m} \quad 2$$

2) The self-weight of the diaphragm

For the edge beam :

$$0.12 + 0.20 \quad 1.60 - 0.20 \quad 0.15 + 0.16 \quad \{ (1 - ()) \times () \times () \times 5 \times 25 \} \quad 2 \quad 22 \quad g2 = 21.50 []$$

$$g2 = 0.529 \text{ kN/m}$$

For the main beam :

$$g' \quad 2 = 2 \times 0.529 = 1.058 \text{ kN/m}$$

3) Bridge deck pavement

$$g_3 = [0.02 \times 7 \times 23 + (2 \times (0.08 + 0.16) \times 7 \times 24) \times 1.5] = 4.676$$

4) Concrete crash wall/Railing and pedestrian

$$g_4 = 5 \times 2 = 2 \text{ kN/m}$$

5) Total

Side girders :

$$g = g_1 + g_2 + g_3 + g_4 = 13.35 + 0.529 + 4.676 + 2 = 20.56 \text{ kN/m}$$

Medium main beam :

$$g = g_1 + g'_2 + g_3 + g_4 = 13.35 + 1.058 + 4.676 + 2 = 21.08 \text{ kN/m}$$

Suppose the distance between the position of the cross section and the fulcrum is x . Therefore, the internal force generated by the dead load of the main beam is as follows:

$$g_x M_x = (1 - x) \times 2 \quad g Q_x = (1 - 2x) \times 2$$

For edge beam :

$$20.56 \times x = 0 \rightarrow Q_0 = 21.50 \text{ kN}, \quad 2 M_0 = 0 \text{ kN} \cdot \text{m}$$

$$1 \times 20.56 \times 21.50 \times x = \rightarrow Q_1 = (21.50 - 2 \times x) = 110.51 \text{ kN} \quad 4 \times 21.50 \times 21.50 \times M_1 = \times \times (21.50 - x) = 890.99 \text{ kN} \cdot \text{m} \quad 4 \times 21.50 \times x = \rightarrow Q_1 = 0 \quad 2 \times 21.50 \times M_1 = \times 20.56 \times 21.50^2 = 1187.98 \text{ kN} \cdot \text{m}$$

Table 4. 3 Edge girders

$$\text{Section Position Shear Force } Q \text{ (kN) Moment } M \text{ (kN} \cdot \text{m)} \quad x = 0 \quad 221.02 \quad 0 \quad 1 \quad x = 110.51 \quad 890.99 \quad 4 \quad 1 \quad x = 0 \quad 1187.98$$

2

For middle beam:

$$21.08 \times x = 0 \rightarrow Q_0 = 21.50 \text{ kN}, \quad 2 M_0 = 0 \text{ kN} \cdot \text{m} \quad 1 \times 21.08 \times 21.50 \times x = \rightarrow Q_1 = (21.50 - 2 \times x) = 113.31 \text{ kN} \quad 4 \times 21.50 \times 21.50 \times M_1 = \times \times (21.50 - x) = 913.27 \text{ kN} \cdot \text{m} \quad 4 \times 21.50 \times x = \rightarrow Q_1 = 0 \quad 2 \times 21.50 \times M_1 = \times 21.08 \times 21.50^2 = 1218.15 \text{ kN} \cdot \text{m}$$

$$113.31 \text{ kN} \quad 4 \times 21.50 \times 21.50 \times M_1 = \times \times (21.50 - x) = 913.27 \text{ kN} \cdot \text{m} \quad 4 \times 21.50 \times x = \rightarrow Q_1 = 0 \quad 2 \times 21.50 \times M_1 = \times 21.08 \times 21.50^2 = 1218.15 \text{ kN} \cdot \text{m}$$

Table 4. 4 Middle beam

$$\text{Section Position Shear Force } Q \text{ (kN) Moment } M \text{ (kN} \cdot \text{m)} \quad x = 0 \quad 226.61 \quad 0 \quad 1 \quad x = 113.31 \quad 913.27 \quad 4 \quad 1 \quad x = 0 \quad 1218.15$$

2

4.2 Calculation of internal forces under live load

1) This is for Beam 1 :

Figure 4. 2 Cross-sectional belonging to the primary beam

Transverse distribution - Eccentric pressure method

a) The span method

$$1 \times 21.50 = 3.07 \geq 2, \text{ eccentric pressure method applies B7}$$

b) Identical for $\eta = 5T$ girders with the distanced at 1.60 m and then :

$$\text{Where : } a_1 = 1.6 \times 2 = 3.2 \text{ m } a_2 = 1.6 \text{ m } a_3 = 0 \text{ m } a_4 = 1.6 \text{ m } a_5 = 1.6 \times 2 = 3.2 \text{ m } \sum a_i^2 = a_1^2 + a_2^2 + a_3^2 + a_4^2 + a_5^2 = (3.2)^2 + (1.6)^2 + 0 + (1.60)^2 + (3.2)^2 = 25.60 \text{ m}^2 \quad \sum a_i^2 = 25.60 \text{ m}^2 \quad 5 \quad i=1 \quad 5 \quad i=1$$

c) Calculating values of influences line of the beam 1

If the section of each beams is the same :

$$1 \times a_{ik} \quad \eta_{ik} = R_{ik} = R_{ik} = \eta \pm \sum_{n=1}^i a_{2i} \quad 1 \times a_{ik} \quad 1 \times (2 \times 1.60)^2 \quad \eta_{11} = \pm \quad i \quad 2 = + = 0.60 \quad \eta \quad \sum_{n=1}^i a_{2i} \quad 5 \quad 25.60 \quad 1 \times a_{ik} \quad 1 \times (2 \times 1.60) \times 1.60 \quad \eta_{12} = \pm \quad i \quad 2 = + = 0.40 \quad \eta \quad \sum_{n=1}^i a_{2i} \quad 5 \quad 25.60$$

$$1 \times a_{ik} \quad 1 \times 0 \quad \eta_{13} = \pm \quad i \quad 2 = + = 0.20 \quad \eta \quad \sum_{n=1}^i a_{2i} \quad 5 \quad 25.60 \quad 1 \times a_{ik} \quad 1 \times (2 \times 1.60) \times (-1.60) \quad \eta_{14} = \pm \quad i \quad 2 = + = 0 \quad \eta \quad \sum_{n=1}^i a_{2i} \quad 5 \quad 25.60 \quad 1 \times a_{ik} \quad 1 \times (2 \times 1.60)^2 \quad \eta_{15} = \pm \quad i \quad 2 = - = -0.20 \quad \eta \quad \sum_{n=1}^i a_{2i} \quad 5 \quad 25.60$$

So the transverse distribution influence of beam 1 and the least at load arrangement of the vehicle in the figure below :

Figure 4. 3 Transverse distribution influence line beam 1 (5)

For beam 1 : $\eta_{11} = 0.6, \quad \eta_{15} = -0.2$ d) Place the most adverse live load and calculated the distance x :

$$x \times 4 \times 1.6 - x = 0.6 \quad 0.2 \quad 0.2x = 0.6 \quad (6.4 - x) \quad 0.2x = 3.84 - 0.6 \times 0.8x = 3.84 \quad x = 4.80 \text{ m}$$

the distance from sidewalk curb to axis of beam 1 :

$$\Delta = 105 - 75 = 30 \text{ cm} = 0.30 \text{ m}$$

e) Calculate m_{cq} and m_{cr} for beam 1 :

$$\text{Pedestrian load } m_{0r} = \sum \eta_i \quad \eta_r \quad 0.6 = 4.8 + 0.3 + 0.75 \quad 4.8 \quad 2 \quad m_{cr} = \eta_r \quad 0.6 \times (4.8 + 0.3 + 4.5 \quad 0.75 \quad 2)$$

$$\text{Vehicle load } m_{0q} = \sum \eta_i \quad 2 \quad \eta_{q1} = 0.6 \quad 1.8 + 1.3 + 1.5 \quad 4.8 \quad \eta_{q1} = 0.575 \quad 4.8 \quad 0.6 \quad (1.8 + 1.3 + 1.5) \quad \eta_{q2} \quad 0.6 = 1.3 + 1.5 \quad 4.8 \quad \eta_{q2} = 0.350 \quad 4.8 \quad 0.6 \quad (1.3 + 1.5) \quad \eta_{q3} \quad 0.6 = 1.5 \quad 4.8 \quad \eta_{q3} = 0.188 \quad 4.8 \quad 0.6 \times 1.5 \quad \eta_{q4} \quad -0.2 = 0.3 \quad 1.6 \quad \eta_{q4} = -0.038 \quad 1.6 \quad -0.2 \times 0.3 = 0.684$$

So, we can get :

$$1 \times m_{cq} = \sum \eta_q = \times (\eta_{q1} + \eta_{q2} + \eta_{q3} + \eta_{q4}) \quad 2 \quad 1 \quad m_{cq} = \times (0.575 + 0.350 + 0.188 - 0.038) = 0.538 \quad 2$$

2) For the beam 2

Figure 4. 4 Cross-sectional of the main beam

a) The span method

1 $21.50 \text{ B7} = 3.07 \geq 2$, eccentric pressure method applies b) Identical for $\eta = 5T$ girders with the

distanced at 1.60 m and then : Where : $a_1 = 1.6 \times 2 = 3.2 \text{ m } a_2 = 1.6 \text{ m } a_3 = 0 \text{ m } a_4 = 1.6 \text{ m } a_5 = 1.6 \times 2 = 3.2 \text{ m}$

$$\sum_{i=1}^5 a_{2i} = a_{12} + a_{22} + a_{32} + a_{42} + a_{52} = (3.2)^2 + (1.6)^2 + 0 + (1.60)^2 + (3.2)^2 \quad \sum a_2 = 25.60 \text{ m}^2 \quad i=1 \text{ to } 5$$

c) Calculating values of influences line of the beam 1

If the section of each beams is the same :

$$\begin{aligned} 1 \text{ a) } \eta_{1k} &= R_{1k} = R_{ik} = \eta \pm \sum_{i=1}^n a_{2i} \quad 1 \text{ a) } \eta_{21} = \pm \frac{1.6}{25.60} = 0.0625 \quad \eta_{22} = \pm \frac{1.6}{25.60} = 0.0625 \quad \eta_{23} = \pm \frac{0}{25.60} = 0 \quad \eta_{24} = \pm \frac{1.6}{25.60} = 0.0625 \quad \eta_{25} = \pm \frac{3.2}{25.60} = 0.125 \\ 1 \text{ a) } \eta_{1k} &= R_{1k} = R_{ik} = \eta \pm \sum_{i=1}^n a_{2i} \quad 1 \text{ a) } \eta_{21} = \pm \frac{1.6}{25.60} = 0.0625 \quad \eta_{22} = \pm \frac{1.6}{25.60} = 0.0625 \quad \eta_{23} = \pm \frac{0}{25.60} = 0 \quad \eta_{24} = \pm \frac{1.6}{25.60} = 0.0625 \quad \eta_{25} = \pm \frac{3.2}{25.60} = 0.125 \end{aligned}$$

So the transverse distribution influence of beam 2 and the least at load arrangement of the vehicle in the figure below :

Figure 4. 5 Transverse distribution influence line of beam 2 (5)

For beam 2 : $\eta_{21} = 0.40$, $\eta_{25} = 0$ d) Place the most adverse live load $\max(\eta_i)$

Figure 4. 6 Schematic diagram of vehicle and pedestrian load

e) Calculate the distance x :

$$x = 160 \times 4 = 640 \text{ cm}$$

the distance from sidewalk curb to axis of beam 2 :

$$\Delta = 105 - 75 = 30 \text{ cm} = 0.30 \text{ m} \text{ f) Calculate } m_{cq} \text{ and } m_{cr} \text{ for beam 2 :}$$

Pedestrian load

$$m_{0r} = \sum \eta_i \quad \eta_r = 0.4 = \frac{640 + 30}{640 + 75} = 0.442$$

Vehicle load

$$\begin{aligned} 1 \text{ m) } m_{0q} &= \sum \eta_i \quad \eta_{q1} = 0.40 = \frac{640 - (50 - 30)}{640} = 0.3875 \quad \eta_{q2} = 0.4 = \frac{160 \times 4 - (20 + 180)}{640} = 0.275 \quad \eta_{q3} = 0.4 = \frac{160 \times 4 - (180 + 20 + 130)}{640} = 0.19375 \quad \eta_{q4} = 0.4 = \frac{160 \times 4 - (180 + 20 + 130 + 180)}{640} = 0.08125 \end{aligned}$$

So, we can get :

$$1 \text{ m) } m_{cq} = \sum \eta_q = 0.3875 + 0.275 + 0.19375 - 0.08125 = 0.775$$

3) Calculation of transverse distribution coefficient by lever method

According to the specifications set, the lever principle method is used on the pedestal to determine the value of the transverse distribution coefficient on the pedestal. By following the following steps:

Figure 4. 7 Lever method applied transverse loading of beam 1 & beam 2

a) Determine the transversal distribution coefficient for beam 1 & 2 b) Draw the influence line for beam 1 & 2 c) The distance from sidewalk curb to axis of beam 1 & 2 : $\Delta = 105 - 75 = 30 \text{ cm}$

Figure 4. 8 Lever method applied to transverse loading of beam 1 & beam 2

Calculation the value of influence line according to the load position

1. Girder 1:

$$\text{Vehicle load : } \eta_q = \frac{160 - (50 - 30)}{160} = 0.875$$

$$160 + (105 - 75) + 75 \text{ Pedestrian load : } \eta_r = \frac{2}{2} = 1.422$$

2. Girder 2 :

$$\text{Vehicle load : } \eta_q = 1.0$$

$$\text{Pedestrian load : } \eta_r = 0.0 \text{ d) Calculate lateral load distribution factor } m$$

1. Girder 1, m :

$$\eta_q = 0.875 \text{ Vehicle load : } m_{0q} = \frac{1}{2} = 0.438$$

$$\text{Pedestrian load : } m_{0r} = \eta_r = 1.422$$

2. Girder 2, m :

$$\eta_q = 1 \text{ Vehicle load : } m_{0q} = \frac{1}{2} = 0.50$$

$$\text{Pedestrian load : } m_{0r} = \eta_r = 0$$

4) Internal force of main beam

The design of RC simply supported beam bridge with five girders, with the span 21.5. Considering the vehicle loads as defined by Highway grade I standard, based on a uniform load design value of : $q_k = 10.5 \text{ kN/m}$, along with a prescribed range for point loads spanning from $P_k = 270 - 360 \text{ kN}$. Determine the peak flexural moment and shear load located at the center related to beam's span, along with highest shear force near the support zone of the side

Figure 4. 9 Longitudinal section

girder. a) Calculation m of the main beam :

1. In the middle span : eccentric pressure method (reliable transverse connections)

$$1 \text{ m) } 21.50 = 2.69 \geq 2 \times 1.60$$

2. Supporting area : lever principal method

$$1 \text{ m) } 21.50 = 2.69 \geq 2 \times 1.60$$

3. Vehicle load :

$$m_c = 0.538 \text{ (middle span)} \quad m_0 = 0.438 \text{ (support area)}$$

4. Pedestrian load :

$m_c = 0.684$ (middle span) $m_0 = 1.422$ (support area)

Table 4. 5 Load variation comparison according to transverse load distribution factors

mcr Girder 1 **mcq** The lever method 0.438 1.422 Eccentric pressure method 0.538 0.684 Girder 2 **mcq** **mcr**

0.50 0 0.469 0.442

b) Determine the lane load and pedestrian load Vehicle load is made up of lane load and automobile load.

1. Load on the lane

Applied in the analysis of an integral bridge structure, the loading scheme incorporates both distributed and concentrated loads in accordance with Highway Grade I specifications :

Figure 4. 10 Loads from vehicular lanes and pedestrian traffic

Characteristic value of uniformly distributed load : $q_k = 10.5$ kN/m Characteristic amount of the applied point force : $P_k = 270 - 360$ kN Notes:

•To account for shear effect, the characteristic concentrated load P_k is adjusted by applying a multiplication factor of 1.2.

•The characteristic values of Highway Grade II : q_k and P_k should be 0.75 times of Highway Grade I.

c) Calculated the lane load and the pedestrian load of Highway I :

1. For $l = 21.50$ m, concentrated load of lane load in the Highway-I.

2. Calculation of moments :

$21.5 - 5 P_k = (270 + (360 - 270) \times) = 303$ kN $50 - 5$

3. Calculation of shears :

$P_k = 1.2 \times 303 = 363.60$ kN

4. The uniform load of the lane load (Highway-I)

$q_k = 10.5$ kN/m

5. Pedestrian load : 3 kN/m d) Calculate areas or values of influence lines of internal forces

Table 4. 6 Influence line of internal forces

Type Section M1 2 Q1 2 Q0 Highway-I (kN/m) 10.5 10.5 10.5 Pedestrian (kN/m) 3 3 3 Area of the I.L (m^2 or m)

$\Omega = 1 = \times 21.52$ 88 11 2 = 57.78 m^2 $\Omega = \times \times 21.5 \times 0.5$ 11 22 = 2.688 m^2 $\Omega = \times 21.5 \times 1$ 1 2 = 10.75 m^2

Influence line

e) Calculate the impact factor

1. Single beam

$A = 0.3902$ m^2

$I_c = 0.066146$ m^4 (moment of inertia for mid - span section)

$G = 0.3902 \times 25 = 9.76$ kN/m

G 9.76 $m_c = = = 0.995$ kN. s^2/m^2 g 9.81

2. C30 : $E = 3.00 \times 10^{10}$ N/ m^2

3. Fundamental frequency

$\pi E I_c$ 3.14 3.00 $\times 10^{10} \times 0.066146$ $f = \sqrt{ } = \sqrt{ } = 4.79$ (Hz) 21.2 m_c 2 $\times 21.52$ 0.995 $\times 10^3$

4. Impact factor

$\mu = 0.1767 \ln f - 0.0157 = 0.276$ $1 + \mu = 1 + 0.276 = 1.276$ f) Calculate maximum moments and shears of the middle span 2 lanes then, $\xi = 1$ Vehicle load : $S_q = (1 + \mu) \times \xi \times (m_i q_k \Omega + m_i P_{kyi})$ Pedestrian load : $S_r = m_i q_k \Omega$ Where : $(1 + \mu)$: The dynamic factor S : The moment or the shear of the calculated section ξ : Lane reduction factor of multi-lane bridge m_i : Lateral load distribution factor q_k : The reference value of the uniform load per meter (load on the lane) P_k : The reference value of the concentrated load (load on the lane) Ω : The influence line area associated with both bending moment and shear force responses y_i : Value on I.L of internal forces according to loads location q_r : Standard value of pedestrian load P.

指 标

疑似剽窃文字表述

1. - 0.20 $\eta \sum_{n=1}^5 a_i = 25.60$

So the transverse distribution influence of beam 1 and the least at load arrangement of the vehicle in the figure below :

Figure 4. 3 Transverse distr

2. .20) $\eta_{25} = \pm i_{25} = 0$ $\eta \sum_{n=1}^5 a_i = 25.60$

So the transverse distribution influence of beam 2 and the least at load arrangement of the vehicle in the figure below :

Figure 4. 5 Tr

3. teristic amount of the applied point force : $P_k = 270 - 360$ kN Notes:
•To account for shear effect, the characteristic concentrated load P_k is adjusted by applying a multiplication factor of 1
4. $1010 \times 0.066146 f = \sqrt{\quad} = \sqrt{\quad} = 4.79(\text{Hz})$ $212 \text{ mc } 2 \times 21.52 0.995 \times 103$
4. Impact factor
 $\mu = 0.1767 \ln f - 0.0157 = 0.276$ $1 + \mu = 1 +$

| | | |
|--|--|-------------------------|
| 4. Scheme design and calculation of Liuquan Medium bridge on Rongwu highway_第4部分 | | 总字数: 16007 |
| 相似文献列表 | | |
| 去除本人文献复制比: 32%(5127) 去除引用文献复制比: 32%(5127) 文字复制比: 32%(5127) 疑似剽窃观点: (0) | | |
| 1 | Scheme Design and Structural Calculation of Chayuan middle-span bridge on Rongwu Highway NAURA BERLIAN HUMAIROH - 《大学生论文联合比对库》- 2024-06-14 | 23.1% (3694) 是否引证: 否 |
| 2 | Scheme design and calculation of Xiaoxin River Middle-span bridge on Rongwu highway YERIBU PROSPER AWOLEBA - 《大学生论文联合比对库》- 2024-07-02 | 16.7% (2672) 是否引证: 否 |
| 3 | Scheme Design and Structural Calculation of Da' angou Medium Bridge in the Zaohe Section of Jinan-Weishan Highway KAUNDE GETRUDE WILLARD - 《大学生论文联合比对库》- 2023-07-12 | 12.7% (2034) 是否引证: 否 |
| 4 | Scheme Design and Structural Calculation of Da' angou Medium Bridge in the Zaohe Section of Jinan-Weishan Highway KAUNDE GETRUDE WILLARD - 《大学生论文联合比对库》- 2023-06-15 | 12.1% (1931) 是否引证: 否 |
| 5 | Scheme Design and Structural Calculation of Yang' jiahe Medium Bridge in the Zaohe Section of Jinan-Weishan Highway HATIM SAFA - 《大学生论文联合比对库》- 2023-06-15 | 11.2% (1789) 是否引证: 否 |
| 6 | Scheme design and calculation of Wangcun Middle-span bridge on Rongwu freeway M. FAREL ASHROFIE - 《大学生论文联合比对库》- 2024-06-26 | 9.9% (1578) 是否引证: 否 |
| 7 | 国际班桥梁-Design of Sanhe Bridge 代超 - 《大学生论文联合比对库》- 2021-06-21 | 0.4% (62) 是否引证: 否 |
| 原文内容 | | |

Table 4. 7 Maximum moments and shears of the middle span
qk or **S** (kN•m Load Section **qr Pk(kN)** ($1 + \mu$) **mi Ω or y** Or kN) Type (kN/m) **Si** S 57.78416.29 Highway-I10.5
303 1.2760.538 1533.65 M1 5.3751117.36 2 Pedestrian 3 - - 0.64857.78 112.29 2.688 19.37 Highway-I10.5
363.601.2760.538 144.03 Q1 0.5 124.66 2 Pedestrian 3 - - 0.6482.688 5.23
How to get Si and S :
 $S_i = (1 + \mu) \times \xi \times (miqk\Omega)$ $S = S_q + sr$ $S = S - S_i$
1. For M1: $2 S = (1 + \mu) \times \xi \times (miqk\Omega + miPkyi)$ $S = 1.276 \times 1 \times ((0.538 \times 10.50 \times 57.78) + (0.538 \times 303 \times 5.375))$ $S = 1533.65$ kN • m Highway I : $Si1 = (1 + \mu) \times \xi \times (miqk\Omega)$ $Si1 = (1.276 \times 1 \times (0.538 \times 10.5 \times 57.78)) = 416.29$ kN • m $Si2 = 1533.65 - 416.29 = 1117.36$ kN • m Pedestrian Load : $Si = miqk\Omega = 0.648 \times 3 \times 57.78 = 112.29$ kN • m 2. For Q1: $2 S = (1 + \mu) \times \xi \times (miqk\Omega + miPkyi)$ $S = 1.276 \times 1 \times ((0.538 \times 10.50 \times 2.688) + (0.538 \times 363.60 \times 0.5))$ $S = 144.03$ kN Highway I : $Si1 = (1 + \mu) \times \xi \times (miqk\Omega) = 1.276 \times 1 \times (0.538 \times 10.5 \times 2.688) = 19.37$ $Si2 = 144.03 - 19.37 = 124.66$ kN Pedestrian Load : $Si = miqk\Omega = 0.648 \times 3 \times 2.688 = 5.23$ kN
a) Calculate maximum shears of the support point

Figure 4. 11 Modification of the transverse distribution coefficient u

1. Length of variation of transverse distribution factor :
 $21.5 - (5.35 \times 4) a = 5.35 + () = 5.4$ m 2
2. Influence line magnitude at the center across the varying segment (m) :
 $1 y = 1 \times (21.5 - \times 5.4) / 21.5 = 0.916$ 3
3. Then,
 $a Q0q = (1 + \mu) \times \xi \times qk [mc\Omega + (m0 - mc)y]$ 2 5.4 $Q0q = 1.289 \times 1 \times 10.5 [0.58 \times 9.75 + (0.438 - 0.538) \times 0.916]$ 2 $Q0q = 73.19$ kN
 $QOP = (1 + \mu) \times \xi \times miPkyi$ $QOP = 1.276 \times 1 \times 0.438 \times 363.60 \times 1$ $QOP = 23.21$ kN

So, the maximum shear force of girder 1, under Highway-I :

$$Q_0 = Q_{0q} + Q_{0p} = 73.19 + 203.21 = 276.4 \text{ kN}$$

4. The maximum shear force of girder 1, under pedestrian load :

$$a \text{ } Q_{0q} = m_{cqr} \Omega + (m_0 - m_c) q_r \cdot y^2$$

$$5.4 \text{ } Q_{0q} = 0.64 \times 2.25 \times 9.75 + \times (1.422 - 0.684) \times 2.25 \times 0.916^2 \text{ } Q_{0q} = 18.15 \text{ kN}$$

Table 4. 8 Maximum shear force of girder 1

qk or **S** (kN) Load Section **qr** **Pk(kN)** (**1 + μ**) **m0 Ω** or **y** Type **Si** **S** (Kn/m) Highway- 9.75 73.19 10.5 299

1. 2760.438 276.4 Q_0 I 1 203.21 Pedestrian 3 - - 1.4229.75 18.15

b) Internal forces combinations

After obtaining internal forces self weight, vehicle loads and pedestrian loads, so as follows :

Table 4. 9 Internal forces combinations

Ultimate

Limit

state

Fundamental

combination

Accidental

Combination

Self weight

is adverse to

the bearing

capacity

Self-weight

is beneficial

to the

bearing

capacity

Frequent

Value

Quasi -

Permanent

Value

Serviceability Frequent Combination

Limit state

Accidental Combination

$$S_{ud} = 1.2G + 1.4Q_v + 0.75 \times 1.4Q_p$$

$$S_{ud} = G + 1.4Q_v + 0.75 \times 1.4Q_p$$

$$S_{ud} = G + 0.7Q_v + 1.0Q_p$$

$$S_{ud} = G + 0.4Q_v + 0.4Q_p$$

$$S_{fd} = G + 0.7Q_v (\text{without impact force})$$

$$+ 1.0Q_p$$

$$S_{qd} = G + 0.4Q_v (\text{without impact force})$$

$$+ 0.4Q_p$$

c) Internal combinations

The calculation of design internal forces (side beam) Table 4. 10 Internal Combinations

Moment M (kN•m)

Shear force Q (kN)

No

Load

1

1

1

$x=0$

$x=$

$x=$

$x=0$ $x =$

4

2

2

1

Self weight

0
913.271218.15226.61 0
2
Vehicle load 0
767.421533.65276.4 144.03
3
Pedestrian load 0
54.9
112.2918.15 5.23

4
1.2 x (1)
01095.9241461.78271.932 0
5
1.4 x (2)
01074.3882147.11386.96 201.642
60.75 x 1.4 x (3) 0
57.645117.90519.058 5.492
7Sud = (4) + (5) + (6) 02227.957 3726.795 677.950 207.134

4.3 Reinforcement design and strength checking calculation

Reinforcement in each main girder is designed by adjusting the results of the internal force analysis in accordance with table 4.10, having the aim of facilitating the construction process.

4.3.1 Principal longitudinal reinforcement arrangement

According to the maximum bending moment of (3726.795 kN • m) in accordance with table 4.10, reinforcement will be organized accordingly. Taking into account the 4 cm net thickness of the steel reinforcement, measurement of main beam's transverse section are presented below :

1) The first stage is to identify the type of T section, provide an approximate measurement of the distance from the force's center of gravity acting on the steel bar to the closest section $a_g = 20$ cm, and then determine the effective height of the girder $h_0 = 155 - 20 = 135$. Assuming h'_i (h'_i where the flange thickness is located in the compressive area of the T section, take $h'_i = h_l$), choose a specific value for determined the bending moment capacity of the section.

$$1 \ h'_i \leq 160 \quad 1 \ Rab'_i (h_0 -) = \gamma_c \times 14.30 \times 1600 \times 160 \times (1350 -) \times \gamma_c \times 1.25 \times 104 \geq 3719.37 \text{ kN} \cdot \text{m} \geq 3726.795 \text{ kN} \cdot \text{m}$$

This is $x \leq h'_i$ includes the first type of the shape part T.

Figure 4. 12 Main beam cross-section measurement (cm)

2) Calculating the height of the concrete compression zone x , as follows :

$$1 \ h'_i \quad M_j = Rab'_i (h_0 -) \quad \gamma_c \times 2 \times \gamma_c M_j x = h_0 - \sqrt{h_0^2 - Rab'_i \times 1.25 \times 3726.795 \times 106} \quad x = 1350 - \sqrt{1350^2 - 14.30 \times 1600 \times 3726.795 \times 106} = 160.34 \text{ mm} = 16.034 \text{ cm} \leq h'_i = 13.5 \text{ cm}$$

$$15.40 \text{ cm} \leq \xi_j h_0 = 0.55 \times 135 = 74.25 \text{ cm} \quad 11781$$

3) Calculating area of cross-section of the tensile steel reinforcement, as follows :

$$Rab'_i \times 14.30 \times 160 \times 16.034 \quad A_g = = = 111.17 \text{ cm}^2 \quad R_g \geq 330$$

24#25, steel bar is selected, area of the section

$$A_g = 24 \times \pi \times 1.25^2 = 117.75 \text{ cm}^2 \geq 111.17 \text{ cm}^2$$

In this Figure 4.11, The reinforcement layout is shown along with the location of the center of gravity of the reinforcement.

$$a'_g \quad y'_g = \sum \sum a'_g \quad (5.4 \times 3.45 \times (7.50 + 6.50 + 5.50 + 4.50 + 3.50 + 2.50 + 1.50 + 0.50)) \quad y'_g = \{ \} \times 5.4 \quad y'_g = 13.80 \text{ cm}$$

Thus, the distance between the point of force application on the reinforcement and the nearest edge of the section is :

$$A_g = 7 + 13.80 = 20.80$$

$$\text{Then, effective height of main beam : } h_0 = 155 - 20.80 = 134.2 \text{ cm}$$

Ratio of reinforcement :

$$\mu = A_g = 111.17 = 0.00517 \geq 0.15\% \text{ so its meet the requirements } b'_i \times h_0 \geq 160 \times 134.2$$

4) Cross-sectional strength analysis

According to the effective area of reinforcement $A_g = 111.17 \text{ cm}^2$ of the section, the height of the concrete compression zone can be calculated, as follows :

$$R_g A_g \geq 330 \times 111.17 \times = = 16.03 \text{ cm}, \text{ Rgis the design tensile strength of grade II steel } R_{bi} \quad 14.30 \times 160 \text{ bar.}$$

Next, the bending strength of the section is :

$$1 \times M_p = Rab'_i \times (h_0 -) \quad \gamma_c \times 2 \times 160.3 \quad 1 \ M_p = 1.25 \times 14.30 \times 1600 \times 160.3 \times (1342 - 2) \times 106 \quad M_p = 3702.43 \text{ kN} \cdot \text{m} \geq M_j = 3726.795 \text{ kN} \cdot \text{m}$$

So, according to this reinforcement main beam it is relatively safe.

4.3.2 Arrangement of shear reinforcement

According to the table 4.10 the maximum design shear force occurs at the fulcrum $Q_0 = 677.950$ kN, in the span $Q_1 = 207.134$ kN. It assumed that $4\phi 25$ longitudinal bars pass through the fulcrum. Therefore, sectional area at support are $A_g = 7 + 3.45 = 10.45$ cm, and the effective depth of the beam become $h_0 = 155 - 10.45 = 144.55$ cm In accordance with the standard beam structure requirements, the section must satisfy the following conditions:

$$Q_j \leq 0.051 \sqrt{R_b} h_0 \quad 0.051 \sqrt{R_b} h_0 = 0.051 \times \sqrt{30} \times 20 \times 144.55 = 807.57 \geq Q_0 = 677.950 \text{ kN}$$

And then the size and section of the beam meet the requirements, if the following formula is satisfied according to the specifications code, and the beam section can only be configured on structural requirements :

$$Q_j \leq 0.038 R_{1b} h_0, \text{ is } R_{1b} \text{ the design tensile strength of C30 concrete.}$$

For the fulcrum section :

$$0.038 R_{1b} h_0 = 0.038 \times 1.43 \times 20 \times 144.55 = 157.10 \text{ kN} \leq Q_0 = 677.950 \text{ kN}$$

$$\text{For mid-span sections : } h_0 = 134.2 \text{ cm } 0.038 R_{1b} h_0 = 0.038 \times 1.43 \times 20 \times 134.2 = 145.85 \leq Q_1 = 207.134$$

Therefore, the configuration of stirrups near the mid-span of the beam can be designed primarily according to structural demands, while for other beam sections, the shear capacity of the inclined plane needs to be assessed. The design for shear reinforcement in the inclined section is shown in this figure 4.13.

1) Calculating the length of various reinforced beams

Assumed that the length of the beam section with the reinforcement according to the structure be x , as follows :

$$x \quad 207.134 - 147.91 = 975 \quad 677.950 - 207.134 \quad x = 0.126 \quad 975 \quad x = 12.285 \text{ cm}$$

Therefore, the beam segment length l_1 of the designed shear reinforcement, as follows :

$$l_1 \quad 2150 \quad l_1 = - x = - 12.285 = 1062.715 \text{ cm } 22$$

According to the code, the maximum shear force appears at a distance of $h/2$ (the beam's height) from the center of the support. At this part, stirrups and concrete resist 60% of the shear load and the remaining 40% is carried by bent steel bars, bending to a 45° angle. Thus we can compute the shear at this location Q'_j , as :

$$Q'_j = Q_0 - \Delta Q_j$$

It can be known in the figure 4.13

$$\Delta Q_j Q_0 l_1 = 2 h \quad 1 \quad 2 \quad 2$$

Resolvent :

$$h(Q_0 - Q_1/2) \quad 155 \times (677.950 - 207.134) \quad \Delta Q_j = = = 33.94 \text{ kN } 1 \quad 2150$$

Figure 4. 13 Illustrated the shear reinforcement design for an incliner section (cm) And then :

$$Q'_j = 677.950 - 33.94 = 644.01 \text{ kN}$$

Therefore, the shear force borne by the inclined bar is :

$$0.4 Q'_j = 0.4 \times 644.01 = 257.604 \text{ kN}$$

The shear force supported by stirrups and concrete is :

$$0.6 Q'_j = 0.6 \times 644.01 = 386.406 \text{ kN} \geq 147.91 \text{ kN}$$

Thus, the length of the part of the beam that is only reinforced with stirrup, as opposed to diagonal bars, is equal to :

$$386.406 - 207.134 \quad l' = \times 12.285 - 12.285 = 249.02 \text{ cm } 207.134 - 147.91$$

Therefore, it is necessary to set the length of the beam section of the oblique reinforcement as :

$$l_1 \quad 2150 \quad l'' = - l' - x = - 249.02 - 12.285 = 813.695 \text{ cm } 22$$

2) Diagonal Reinforcement Design

In the top part of the beam, the installed steel bar is 4.5 cm far from the top surface. The bar is bent about 45° , and its horizontal projection along the beams axis is:

$$C = 155 - 4.5 - 6.45 = 144.05$$

The number of rows of diagonal bars n is:

$$l' \quad 813.695 \quad n = = = 5.65 \quad C \quad 144.05$$

The integral value of $n = 5$, refers to five rows of inclined bars. The shear force resisted by the bent bars crossing the diagonal section is given by :

$$Q_w = 0.006 R_{gw} \sum A_{ws} \sin \alpha$$

For the first row of bent bars, the shear force resisted by the diagonal reinforcement located at the distance of half the beam depth $h/2$ from the support is given by $Q_{w1} = 266.482$ kN Cross sectional area required in first row :

$$Q_{w1} \quad 266.482 \quad A_{gw1} = = = 19.036 \text{ cm}^2 \quad 0.06 R_{gw} \sin 45^\circ \quad 0.06 \times 330 \times 0.707$$

Assuming the height h' of the diagonal reinforcement remains constant, the shear force carried by each row of

inclined bars can be determined using the following formula:

$$h' Q_{wi} = Q_{w1} [1 - (2i - 3)] \frac{2C1}{2}$$

In the formula $i = 2, 3, 4, 5 \dots$ h' is the height of the diagonal bar, the value is : $h' = 119\text{cm}$

$$h \frac{155}{C1} = \frac{1' -}{-} = 813.695 - = 736.195 \text{ cm}$$

Therefore, it can be concluded that the calculating shear force resisted by the second, third, and fourth rows of diagonal reinforcement, as well as the required cross-sectional areas of the rebar, as follow:

$$\begin{aligned} 119 Q_{w2} &= 266.482 \times [1 - (2 \times 2 - 3)] \times \frac{2 \times 736.195}{2} = 245.04 \text{ kN} \\ 2 \times 736.195 Q_{w2} &= 245.04 \times 2 \times 736.195 = 358.08 \text{ cm}^2 \\ 0.06 R_{gwsin450} &= 0.06 \times 330 \times 0.707 = 14.43 \text{ cm} \\ 119 Q_{w3} &= 266.482 \times [1 - (2 \times 3 - 3)] \times \frac{2 \times 736.195}{2} = 201.95 \text{ kN} \\ 2 \times 736.195 Q_{w3} &= 201.95 \times 2 \times 736.195 = 296.74 \text{ cm}^2 \\ 0.06 R_{gwsin450} &= 0.06 \times 330 \times 0.707 = 14.43 \text{ cm} \\ 119 Q_{w4} &= 266.482 \times [1 - (2 \times 4 - 3)] \times \frac{2 \times 736.195}{2} = 158.75 \text{ kN} \\ 2 \times 736.195 Q_{w4} &= 158.75 \times 2 \times 736.195 = 232.50 \text{ cm}^2 \\ 0.06 R_{gwsin450} &= 0.06 \times 330 \times 0.707 = 14.43 \text{ cm} \\ 119 Q_{w5} &= 266.482 \times [1 - (2 \times 5 - 3)] \times \frac{2 \times 736.195}{2} = 115.78 \text{ kN} \\ 2 \times 736.195 Q_{w5} &= 115.78 \times 2 \times 736.195 = 170.56 \text{ cm}^2 \\ 0.06 R_{gwsin450} &= 0.06 \times 330 \times 0.707 = 14.43 \text{ cm} \end{aligned}$$

Based on the calculation results, there are two long steel bars (2N2) bent at a 45° angle, which serve as the first row of diagonal reinforcement. The cross-sectional area is only 11.7 cm^2 , which is obviously less than the required 15.705 cm^2 . So, we need to change the spacing of the next row of diagonal reinforcement. So to make up for the shortfall, we added two additional steel bars (2N3) that were also bent at a 45° angle, and placed 65 cm away from the first row. In addition, to increase the shear capacity of the diagonal reinforcement, we also installed two $2\phi 8$ auxiliary angled bars between the bent diagonal bars. For placement details, please refer to figure 4.14.

3) Verification of the flexural strength of the standard section following the bending of the longitudinal reinforcement.

Compute the moment M_{j1} , M_{j2} , and M_j according to the change of parabola. Bending moment envelope diagram was drawn according to the parabolic trend. Then a diagram of the longitudinal flexural capacity will be created, indicating where the steel bar can be bent. The equivalent flexural resistance will be determined $2\phi 25$ rebars :

$$\begin{aligned} x &= 0.099 M = 2 R_g A_g (h_0 - x) = 2 \times 330 \times 103 \times 4.91 \times 10^{-4} \times (1.342 - x) \\ M &= 418.85 \text{ kN} \cdot \text{m} \end{aligned}$$

The total bending moment capacity ΣM contributed by the longitudinal reinforcement at the mid-span section is calculated as follows:

$$0.099 \Sigma M = 330 \times 103 \times 78.54 \times 10^{-4} \times (1.342 - x) = 3349.93 \text{ kN} \cdot \text{m}$$

Figure 4.14 verification of overall flexural capacity of the beam the curvature evolution point for the curved longitudinal reinforcement is so far away from the cross section where the flexural strength calculations indicates that reinforcement is no longer necessary up to h_0 The placement reinforcement meets the design criteria as shown in 2 figure 4.14.

Figure 4. 14 Illustrated the verification of the overall beam' s load bearing capacity

4) Stirrup Design

Based on the ratio of longitudinal tensile reinforcement at the main beam' s support location , where $P = 100 \mu$, Both small and large spans use stirrups as follows : four-leg stirrups of $4\phi 8$ and double-leg stirrup of $2\phi 8$ are selected, respectiley. The corresponding cross-sectional areas are $A_{k4} = 2.012 \text{ cm}^2$ and $A_{k2} = 1.006 \text{ cm}^2$.

The formula for calculating the stirrup spacing is :

$$0.0033 (2 + P) \sqrt{P A_k R_{gk} b h_0} S_k = (Q' / j)^2$$

For the fulcrum, the longitudinal main rib is $5\phi 25$, $A_g = 24.544 \text{ cm}^2$

$$h_0 = 155 - 5 - 3.45 = 146.55 \text{ cm} \quad \mu = \frac{A_g}{b h_0} = \frac{24.544}{20 \times 146.55} = 0.0837$$

$$P = 100 \mu = 8.37$$

$Q' / j = 644.01 \text{ kN}$, Substitute into the formula :

$$0.0033 (2 + P) \sqrt{P A_k R_{gk} b h_0} S_k = (Q' / j)^2 \quad 0.0033 \times (2 + 8.37) \times \sqrt{30 \times 2.012 \times 330 \times 20 \times 146.552} S_{k0} = 128.89 \text{ cm}$$

For the span, longitudinal main rib is $12\phi 32$, $A_g = 78.54 \text{ cm}^2$

$$h_0 = 155 - 17.80 = 137.2 \text{ cm} \quad \mu = \frac{A_g}{b h_0} = \frac{78.54}{20 \times 137.2} = 0.029$$

$$P = 100 \mu = 2.9$$

$Q' / j = 207.134 \text{ kN}$, Substitute into the formula :

$$0.0033 \times (2 + 2.9) \times \sqrt{30 \times 1.006 \times 330 \times 20 \times 137.22} S_{k1} = 257.99 \text{ cm}$$

According to the relevant code provisions, for thin walled flexural members, the stirrup spacing must be less than $\frac{1}{4}$ of the beam height and should not exceed 50 cm . Additionally, within a distance $0.5 h$ on both sides of the support center, the stirrup spacing must not exceed 20 cm . Therefore, the stirrup spacing along the beam is specified as $S_k = 20 \text{ cm}$, except within 10 cm near the support where closer spacing is required. The transition from four-legged to two-legged stirrups occurs at a distance of 3.5 m from the support. The verification of the stirrup reinforcement ratio is as follows : For the fulcrum :

$Ak_4 \frac{2.012}{\mu k_0} = 0.01006 \geq \mu_{Rmin} = 0.0018 \frac{bSk_0}{20 \times 10}$
 $Ak_4 \frac{1.006}{\mu_1} = 0.0025 \geq \mu_{Rmin} = 0.0018 \frac{k_2 bSk_1}{20 \times 20 \times 2}$
5) Verification of shear strength at the inclined section

In accordance with design standards, the shear strength should be evaluated at specific critical points. These include a location situated at a distance of half beam depth ($h/2$) from the support center, at zones where the tensile reinforcement bends particularly where changes occur in the amount or spacing of stirrups and in areas where the web thickness of the bending element differs. The shear strength of the inclined sections is illustrated in figure 4.15.

The section located $h/2$ from the support is designated as section 1-1

Shear force :

$Q_{1-1} = 411.42 \text{ kN}$

Bending moment:

$M_{1-1} = 695.82 \text{ kN}$

3.4 m away from the center of the support is section 5-5, which is the bending starting point of the fourth row of curved steel bars.

Shear force:

$Q_{5-5} = 301.92 \text{ kN}$

Bending moment:

$M_{5-5} = 1646.45 \text{ kN}$

The maximum shear force can be estimated by interpolation after determining the horizontal projection length C of the inclined section. The corresponding bending moment is then obtained proportionally from the bending moment envelope diagram. The calculation horizontal projection length $C \approx h_0$ (available average) of the inclined section, the value of w can be approximated using the average effective height of the section, such that :

| 指 标 |
|-----|
|-----|

疑似剽窃文字表述

- the support point
Figure 4. 11 Modification of the transverse distribution coefficient μ
1. Length of variation of transv
- Pedestrian 3 - - 1.4229.75 18.15
b) Internal forces combinations
After obtaining internal forces self weight, vehicle loads and pedestrian loads, so as follows :
Table 4. 9 Internal forces combination
- $50 + 0.50)) y' = \{ \} 8 \times 5.4 y' = 13.80\text{cm}$
Thus, the distance between the point of force application on the reinforcement and the nearest edge of the section is :
 $A_g = 7 + 13.80 = 20.80$
Then, effective height of main beam : $h_0 = 155$
- $3702.43 \text{ kN} \cdot \text{m} \geq M_j = 3726.795 \text{ kN} \cdot \text{m}$
So, according to this reinforcement main beam it is relatively safe.
4.3.2 Arrangement of shear reinforcement
According to the table 4.10 the maximum design shear force occurs at the fulcrum $Q_0 = 677.950 \text{ kN}$, in the span $Q_1 = 207.134 \text{ kN}$. It assumed that $4\phi 25$ lon
- $44.55 = 807.57 \geq Q_0 = 677.950 \text{ kN}$
And then the size and section of the beam meet the requirements, if the following formula is satisfied according to the specifications code, and the beam section can only be configured on structural requirements :
 $Q_j \leq 0.038 R_{ib} h_0$, is R_{i} the design tensile strength of C30 concrete.
For the fulcrum section :
 $0.038 R_{ib} h_0 = 0.038 \times 1.43 \times 20 \times 144.55 = 157.10 \text{ kN} \leq Q_0 = 677.950 \text{ kN}$ For mid-span sections :
 $h_0 = 134,2 \text{ cm}$ $0.038 R_{ib} h_0 = 0.038 \times 1.43 \times 20 \times 134.2 = 145.85 \leq Q_1 = 207.134 \text{ kN}$
Therefore, the configuration of stirrups near the mid-span of the beam can be designed primarily according to structural demands, while for other beam sections, the shear capacity of the inclined plane needs to be assessed. The design for shear reinforcement in the inclined section is shown in this figure 4.13.
1) Calculating the length of various reinforced beams

- Assumed that the length of the beam section with the rein
6. then :
 $Q' j = 677.950 - 33.94 = 644.01 \text{ kN}$
 Therefore, the shear force borne by the inclined bar is :
 $0.4Q' j = 0.4 \times 644.01 = 257.604 \text{ kN}$
 The shear force supported by stirrups and concrete is :
 $0.6Q' j = 0.6 \times 644.01 = 386.40$
 7. $.036 \text{ cm}^2$ $0.06R_g \sin 45^\circ = 0.06 \times 330 \times 0.707$
 Assuming the height h' of the diagonal reinforcement remains constant, the shear force carried by each row of inclined bars can be
 8. $55 \text{ Cl} = 1' - ' - = 813.695 - = 736.195 \text{ cm}^2$
 Therefore, it can be concluded that the calculating shear force resisted by the second, third, and fourth rows of diagonal reinforcement
 9. ase refer to figure 4.14.
 3) Verification of the flexural strength of the standard section following the bending of the longitudinal reinforcement.
 Compute the moment M_{j1} , M_{j1} , and M_j , according to the change of parabola. Bending 24 moment envelope diagram was drawn according to the parabolic
 10. $20 \times 137.22 \text{ S k}_1 = = 257.99 \text{ cm}^2$ 207.1342
 According to the relevant code provisions, for thin walled flexural members, the stirrup spacing must be less than $\frac{3}{4}$ of the beam height and should not exceed 50 cm. Additionally, within a distance $0.5h$ on both sides of the support center, the stirrup spacing must not exceed 20 cm. Therefore, the stirrup spacing along the beam is specified as $S_k = 2$
 11. ctions is illustrated in figure 4.15.
 The section located $h/2$ from the support is designated as section 1-1
 Shear force :
 $Q_{1-1} = 411.42 \text{ kN}$
 Bending moment:
 $M_{1-1} = 695.82 \text{ kN}$
 3.4 m away from the center of the support is section 5-5, which is the bending starting point of the fourth row of curved steel bars.
 Shear force:
 $Q_{5-5} = 301.92 \text{ kN}$
 Bending moment:
 $M_{5-5} = 1646.45 \text{ kN}$
 The maximum shear force can be estimated by interpolation after determining the horizontal projection length C of the inclined section. The corresponding bending moment is then obtained proportionally

| | | |
|--|--|-------------------------|
| 5. Scheme design and calculation of Liuquan Medium bridge on Rongwu highway_第5部分 | | 总字数: 16548 |
| 相似文献列表 | | |
| 去除本人文献复制比: 21.7%(3595) 去除引用文献复制比: 21.7%(3595) 文字复制比: 21.7%(3595) 疑似剽窃观点: (0) | | |
| 1 | Scheme Design and Structural Calculation of Chayuan middle-span bridge on Rongwu Highway NAURA BERLIAN HUMAIROH - 《大学生论文联合比对库》- 2024-06-14 | 16.0% (2651) 是否引证: 否 |
| 2 | Scheme Design and Structural Calculation of Yang' jiahe Medium Bridge in the Zaohe Section of Jinan-Weishan Highway HATIM SAFA - 《大学生论文联合比对库》- 2023-07-12 | 12.6% (2082) 是否引证: 否 |
| 3 | Scheme Design and Structural Calculation of Da' angou Medium Bridge in the Zaohe Section of Jinan-Weishan Highway KAUNDE GETRUDE WILLARD - 《大学生论文联合比对库》- 2023-07-12 | 11.4% (1879) 是否引证: 否 |
| 4 | Scheme Design and Structural Calculation of Da' angou Medium Bridge in the Zaohe Section of Jinan-Weishan Highway KAUNDE GETRUDE WILLARD - 《大学生论文联合比对库》- 2023-06-15 | 10.8% (1780) 是否引证: 否 |

| | | |
|---|---|-------------------------|
| 5 | Scheme Design and Structural Calculation of Yang' jiahe Medium Bridge in the Zaohe Section of Jinan-Weishan Highway HATIM SAFA - 《大学生论文联合比对库》 - 2023-06-15 | 10.7% (1765) 是否引证: 否 |
| 6 | Scheme design and calculation of Wangcun Middle-span bridge on Rongwu freeway M. FAREL ASHROFIE - 《大学生论文联合比对库》 - 2024-06-26 | 8.6% (1417) 是否引证: 否 |

原文内容

$$146.55 + 137.2 C = 141.875 \text{ CM}^2$$

In cases where the flexural element is strengthened through the reinforcement provided by closed loops and angled reinforcement rods, shear strength of the inclined section is checked using the equation below :

$$Q_j \leq Q_{hk} Q_w$$

In the above formula Q_{hk} represents the combined shear resistance provided by the concrete and stirrups at the inclined section, and is expressed as

$Q_{hk} = 0.0349 b h_0 \sqrt{(2 + P) \times \sqrt{R_{\mu k} R_{gk}}}$, P , μ_k , Q_w are the same meaning as before concrete and stirrup section 1-1

Where : a) P , μ_k and Q_w retain their previously defined meanings b) The parameters are evaluated for section 1-1, where both concrete and stirrup contributions are considered

Reinforcement ratio of longitudinal reinforcement :

$$24.544 P = 100 \mu = 100 \times = 0.865 \frac{20 \times 141.875}{A_k 2.012} \mu_k = = 0.00503 \frac{b S_k 20 \times 20}{Q_{hk} 20 \times 20} Q_{hk} = 0.0349 b h_0 \sqrt{(2 + P) \times \sqrt{R_{\mu k} R_{gk}}}, P, \mu_k, Q_w$$

$$Q_{hk4} = 0.0349 \times 20 \times 141.875 \times \sqrt{(2 + 0.865) \times \sqrt{30 \times 0.00503 \times 330}}$$

$$Q_{hk4} = 505.41 \text{ kN} \quad Q_{w4} = 0.06 \times 330 \times 12.272 \times 0.707 = 171.79 \text{ kN} \quad \text{So, : } Q_{hk4} + Q_{w4} = 505.41 + 171.79 = 677.2 \text{ kN} \geq 411.42 \text{ kN}$$

Figure 4. 15 Illustrated the verification of shear strength in an inclined section

Oblique section 4-4:

The section of longitudinal reinforcement :

$$58.905 P = 100 \mu = 100 \times = 2.076 \frac{20 \times 141.875}{A_k 1.006} \mu_k = = 0.0025 \frac{b S_k 20 \times 20}{Q_{hk4} 20 \times 20} Q_{hk4} = 0.0349 \times 20 \times 141.875 \times \sqrt{(2 + 2.076) \times \sqrt{30 \times 0.0025 \times 330}}$$

The stirrup changes from 4 limbs to 2 limbs in the range of oblique section 4-4:

$$330 Q_{hk4} = 424.997 \text{ kN} \quad Q_{w4} = 0.06 \times 330 \times 12.272 \times 0.707 = 171.79 \text{ kN} \quad \text{So, : } Q_{hk4} + Q_{w4} = 424.997 + 171.79 = 596.787 \text{ kN} \geq 411.42 \text{ kN}$$

Based on design experience, on the conditions that the longitudinal tension reinforcement alongside the transverse ties is arranged in strict accordance with the construction requirements specified by the relevant codes, the flexural strength of the sloped segment may be considered assured without the necessity of further verification calculations.

4.4.2 Crack Verification Calculations

In the case of reinforced concrete flexural components with a T-shaped cross sectional profile, the peak width of cracks can be estimated by utilizing the following expression :

$$\delta g 30 + d \delta f_{\max} = C_1 C_2 C_3 () E_g 0.28 + 10 \mu$$

In which:

C_1 : Consider coefficient of steel bar surface shape for threaded steel bars $C_1 = 1.0$

C_2 : Consider the coefficient of load action, long-term load action $C_2 = 1 + 0.5 M_0 / M$

Where M_0 represents the bending moment caused by long-term loading, while M denotes the bending moment experienced under the full-service load conditions.

C_3 : A coefficient relate to the form of a member, when a flexural member has a web

$$C_3 = 1.0$$

d : Diameter of the longitudinal tensile bar A_g

μ : The ratio of reinforcement is calculated according to the following formula:

$$A_g \mu = , \text{ when } \mu \geq 0.02 \text{ is used the value is } \mu = 0.02 b h_0 + (b_i - b) h_i$$

b_i, h_i : Width and thickness of tension flange

σ_g : Stress of a tensile steel bar under service load, calculate according to the formula :

$$M \sigma_g = 0.87 A_g h_0$$

The following calculation evaluates whether the maximum crack width in the main beam span, under normal environmental conditions and long-term loading with load combination, satisfied the required limits.

$$I [\delta f_{\max}] = 0.2 \text{ mm}$$

Value $C_1 = 1.0$ (threaded steel bar).

Under the action of load combination 1:

$$M_0 670.19 \quad C_2 = 1 + 0.5 = 1 + 0.5 \times = 1.231 \quad M 670.19 + 725.40 + 53.26$$

Value $C3 = 1.0$ (flexural member having web), $d=25$ mm

$$A_g 58.87 \mu = 0.022 \geq 0.020 b h_0 + (b_i - b) h_i 20 \times 137.2$$

Taking $\mu = 0.02$

$$M (670.19 + 725.40 + 53.3) \times 106 \sigma_g = 206.19 \text{ Mpa } 0.87 A_{gh} 0.87 \times 5887 \times 1372 E_g = 2.0 \times 105 \text{ Mpa}$$

So, the load combination is I:

$$206.19 30 + 25 \delta f_{max} = 1 \times 1.231 \times 1 \times ()^2 \times 105 0.28 + 10 \times 0.02$$

$$\delta f_{max} = 0.145 \text{ mm} \leq [\delta f_{max}] I = 0.2 \text{ mm}$$

4.3.3 Main beam deflection verification calculation

The immediate deformation of a reinforced concrete bending member is capable of being determined through material mechanics principles, considering the defined stiffness characteristics of the member.

For simply supported beams :

$$5 M L^2 f = 0.85 E I_{01}$$

In the formula :

L : Calculated span.

M : Bending moment under service load (static and live load bending moment).

I_{01} : The cracked section is converted to the moment of inertia.

$$I_{01} = n A_g (h_0 - x)^2 + b' i, x^3 - (b' i - b) (x - t)^3 33 E_h = 3.0 \times 10^4 \text{ Mpa}, n = 10$$

Determine the sections type of this type, hypothesis $x = h' i = 17.5$ cm

$$I_{01} b' i h' i^2 = 160 \times 17.5^2 = 24500 \text{ cm}^3 \leq n A_g (h_0 - h' i)^2 = 10 \times 58.87 \times (137.2 - 17.5) = 70467.39$$

cm³

Calculation shows $x \geq 17.5$, it belongs to class I T-section

$$x = -A + \sqrt{A^2 + B} n A_g (b' i - b) h_i 10 \times 58.87 + (160 - 20) \times 17.5 A = 151.935 b 20 n A_g (b' i - b) h' i^2 + 2 A_{gh} (160 - 20) \times 17.5^2 + 2 \times 10 \times 58.87 \times 137.2 B = b 20 B = 10220.714 x = -151.935 + \sqrt{137.22 + 10220.714} = 18.48 \text{ cm } I_{01} = 10 \times 58.87 \times (137.2 - 18.48)^2 + 160 \times 18.48^3 - (160 - 20) \times (18.48 - 17.5)^3 I_{01} = 8633942.803 \text{ cm}^4 = 0.0863 \text{ m}^4$$

According to the code, when checking the deformation related to the main girder, dead force is excluded, along with the Highway-Grade I load is calculated without considering the impact factor.

Deformation is caused by the static load, live load, and pedestrian (crowd) load:

$$725.40 5 M L^2 5 \times (1.296 + 53.2) \times 21.52 f = 0.0171 \text{ m } 0.85 E I_{01} 48 \times 0.85 \times 2.35 \times 107 \times 0.0863 L 2150 f = 1.71 \text{ cm} \leq 3.58 \text{ cm } 600 600$$

Deformation check calculation complies with the specification requirements.

As stipulated by the code, when the vertical deflection resulting from the combined effects of gravity load and highway grade I load (excluding impact effect) surpasses one six-hundredth of the span length, the provision of a pre-camber is required. The pre-camber value should correspond to the vertical deflection resulting from the combined gravity load and half of the highway- Grade I load (excluding impact force).

$$725.40 5 M L^2 5 \times (1.296 + 670.19) \times 21.52 f = 0.0269 \text{ m } 0.85 E I_{01} 48 \times 0.85 \times 3 \times 107 \times 0.0863 L 2150 f = 2.69 \text{ cm} \geq 1.343 \text{ cm } 1600 1600$$

The pre-camber should be set with a value of :

$$1 2 1 725.40 5 (M_g + 2 M_{\text{highway-I}}) L^5 \times (670.19 + 2 \times 1.296) \times 21.52 f_y = 48 \times 0.85 E_h I_{01} 48 \times 0.85 \times 3 \times 107 \times 0.0863 f_y = 0.0208 \text{ m} = 2.08 \text{ cm}$$

Hence, it is recommended that the structure be formed into a smooth, continuous curve to maintain both structural integrity and visual harmony.

Chapter 5 Calculations of Diaphragm

5.1 Calculation of diaphragms

In a reinforced concrete beam bridge that does not include transverse beams, it is essential to ensure that the main longitudinal beams act in unison to maintain the structural integrity of the system. This is achieved by providing sufficient stiffness and strength in the transverse beam located at mid-span typically experiences the highest internal forces, as the central region of the span is generally subjected to the most critical and unfavorable loading conditions. Therefore, structural analysis is primarily concentrated on evaluating the internal forces acting on the mid-span transverse beam. The design parameters derived from this analysis are then considered safe for application to other transverse beams, as they are subjected to relatively less severe loading.

Given that the parameters $\theta = 0.301$ and $\sqrt{a} = 0.414$ are obtained from the analysis of the main beam, influence coefficients of the transverse bending moment, denoted as μ_0 and μ_1 , at the midpoint of the bridge width (where the beam position is $f = 0$) can be determined using the G - M method, referring to established tables, $B \mu \alpha$, at the mid-span section of a single-width transverse beam can be calculated, as presented in table 5.1. Due to the symmetry of the influence line data for the range $0 \sim (-B)$ with respect to the range $0 \sim B$, only one side of the data is included in the table 5.1 for brevity.

Consequently, the flexural moment occurring at the center of single width transverse structural member correspond to the coordinate values of the influence line $B\mu\alpha$, which plays a vital role as a reference in structural analysis and designs.

Table 5. 1 Mid-span bending moment influence line coordinates for a single-width transverse member

| | | | | | | | | | | | | | | | | | | | | | | | | | | | | |
|---------------------------|-------|--------|-------|-------|-------|-------|---|-------|-------|--------|--------|--------|--------|-------|-------|-------|--------|--------|---|-------|--------|--------|--------|--------|-------|---|---|---|
| Load Position Calculation | | | | | | | | | | | | | | | | | | | | | | | | | | | | |
| B | 3/4 | B | 1/2 | B | 1/4 | B | 0 | μ | 0 | -0.145 | -0.125 | -0.001 | 0.120 | 0.250 | μ | 1 | -0.100 | -0.045 | | | | | | | | | | |
| 0.025 | 0.110 | 0.220 | μ | 1 | - | μ | 0 | 0.045 | 0.080 | 0.026 | -0.010 | -0.030 | (μ | 1 | - | μ | 0) | √ | α | 0.099 | 0.176 | 0.057 | -0.022 | -0.066 | | | | |
| <hr/> | | | | | | | | | | | | | | | | | | | | | | | | | | | | |
| μ | α | = | μ | 0 | + | (μ | 1 | - | μ | 0) | √ | α | -0.046 | 0.051 | 0.056 | 0.098 | 0.184 | B | μ | 0(m) | -0.653 | -0.563 | -0.005 | 0.540 | 1.125 | B | μ | α |
| <hr/> | | | | | | | | | | | | | | | | | | | | | | | | | | | | |
| x | a(m2) | -1.004 | 1.113 | 1.222 | 2.139 | 4.016 | | | | | | | | | | | | | | | | | | | | | | |

Note : in table $B = 4.5$ m, is half of the bridge width $\alpha = 4.85$ m is the beam spacing.

To assess how vehicular loads influence the bridge's structural behavior, especially in identifying the internal forces on the transverse beam, it is necessary to convert discrete or concentrated loads into an equivalent continuous form. For this purpose, the peak value of a sinusoidal load distribution, which can approximate the influence of multiple concentrated loads, is determined using the following formula as shown :

$$2 \pi x_i P = L \sum P_i \sin \frac{\pi x_i}{L}$$

Where :

P : This refers to the maximum value of the equivalent sinusoidal load applied along the span.

P_i : Represents the magnitude of each individual concentrated load. x_i : The refers to space separating concentrated load P_i along with the baseline, which is usually the support or fulcrum.

L : This is the actual span length of the bridge.

This equation facilitates transformation of a series of concentrated vehicular loads into a smooth sinusoidal loading pattern, which simplifies the analysis of the structural response, especially when evaluating deflections and bending moments in transverse structural elements.

For the purpose of this study, Highway Grade I loading configurations are adopted in accordance with current national bridge design standards. The load arrangement is strategically positioned along the bridge span to produce the maximum internal force in the central transverse beam (crossbeam). This is critical, the central section of the bridge span usually experiences the greatest stress concentration because of the effect of both symmetric and asymmetric loading patterns. The optimal positioning of these loads for maximum transverse beam response is illustrated in figure 5.1.

By applying this method, the analysis ensures a realistic and conservative estimation of the structural behavior under standard vehicular loading conditions,

Figure 5. 1 Distribution of loads along the bridge spans (cm)

Thereby contributing to the safe and efficient design of bridge components.

Peak value of the sinusoidal load caused by the longitudinal wheel load is as follows :

$$2 \pi x_i P = L \sum P_i \sin \frac{\pi x_i}{L} \quad 2 \times 60 \times 6.75 \times 120 \times 10.75 \times 120 \times 9.35 \times P = \times (\sin \frac{\pi}{2} + \sin \frac{\pi}{2} + \sin \frac{\pi}{2}) \quad 21.5 \times 2 \times 21.5 \times 2 \times 21.5 \times 2$$

$$21.5 \times 2 \times P = \times (30 \sin 0.314 \pi + 60 \sin 0.5 \pi + 60 \sin 0.435 \pi) \quad 21.5 \times 2 \times P = \{30 \times 0.834 + 60 \times 1 + 60 \times 0.979\} =$$

$$13.37 \text{ kN/m} \quad 21.5$$

The highest value of the sinusoidal load corresponding to the crowd load is calculated as shown :

$$2 q_r L \pi x \quad 2 q_r L \pi x L \quad P_r = \int \sin dx = [-\cos] \quad L \quad 0 \quad L \quad L \quad \pi \quad L \quad 0 \quad 2 q_r L \quad 4 q_r P_r = (-) = - = 3.82 \text{ kN/m} \quad L \quad \pi$$

$$3.1416$$

5.2 Bending moment calculations of diaphragm

According to the calculation results shown in Table 5.1, influence line diagram for the transverse beam bending moments can be constructed by plotting the product of $B\mu\alpha$ and α . Subsequently, the applied loads are arranged according to the most unfavorable loading configuration in the horizontal direction, presented in Figure 5.2.

Given that the span length of the beam is 21.5 meters and the dynamic impact coefficient $1 + \mu = 1.276$, the bending moment at the mid-span section of the transverse beam, under various loading conditions, can be calculated using the the equation below :

$$M_q = (1 + \mu) \times P_q \sum (B\mu\alpha \times \alpha)$$

Where :

M_q : Flexural force observed at the mid-span on transverse structural member resulting from vehicular traffic induced forces.

$(1 + \mu)$: Dynamic impact coefficient, accounting for the amplification effect from moving loads (vibration, shock). In this case $(1 + \mu) = 1.276$.

P_q : The concentrated load from the vehicle at a specific location (typically in tons or kN).

$\sum (B\mu\alpha \times \alpha)$: A summation of the product of :

• $B\mu\alpha$ = The influence line ordinate associated with the bending force at position α throughout the cross beam.

• α = Load location on the transverse direction, which may indicate the distribution factor or influence

at that specific point.

This equation incorporates the effect of dynamic amplifications cause by moving loads through the impact coefficient, while also considering the influence line values for each load position across the bridge width. The bending moment obtained corresponds to the critical values at the mid-span of the transverse beam, which serves as basis for evaluating the structural capacity and ensuring safe design under the traffic loads.

$$M_q = (1 + \mu) \times P_q \sum (B \mu \alpha \times \alpha) \quad M_{q(+)} = 1.276 \times 13.37 \times (4.016 + 2.139 + 1.6805 + 1.276 + (-0.0545))$$

$$M_{q(+)} = 154.51 \text{ kN/m}$$

$$M_{q(-)} = 1.276 \times 13.37 \times ((-0.0545) + 2.139) = 35.56 \text{ kN/m}$$

$$-1.004 + (-0.0545) \quad M_q = P \lambda \sum B \mu \alpha \times \alpha =$$

$$3.82 \times [\times 2] = -4.04 \text{ kN/m}^2$$

Figure 5. 2 Influence line representing beam bending moments

In the load combination : Due to relatively balanced effect in terms of the beams bending moment, over both the positive and negative segments on influence line, impact of dead load on bending moment is mostly neutralized. As a result, the internal force resulting from the dead load can be neglected in the analysis. Thus, the calculation becomes :

$$M_q = 1.4 M_{q(+)} = 1.4 \times 154.51 = 216.314 \text{ kN/m}$$

Negative moment combination :

$$1.4 M_r = 1.4 \times (-4.04) = -5.656 \text{ kN/m}$$

Accordingly, the resulting internal forces in the beam are : a) The positive bending moment is governed by the Highway - Grade I loading :

$$M(+) = 216.314 \text{ kN/m}$$

b) The negative bending moment is governed by the crowd load :

$$M(-) = -5.656 \text{ kN/m}$$

5.3 Strength and reinforcement verification of diaphragm

a) Positive moment reinforcement :

The pavement layer is idealized as a 3 cm thickness and included in the cross-sectional calculation. Therefore, calculated effective breadth b' of flange plate corresponds to established as illustrated :

$$2\lambda + b = 2 \times 140.8 + 20 = 301.6 \text{ cm} \quad b + 12h_w = 20 + 12 \times (17.5 + 3) = 266 \text{ cm}$$

According to the relevant design specifications, the smaller value is adopted, therefore, $b' = 266 \text{ cm}$.

Assuming the concrete cover $a = 8 \text{ cm}$, the effective depth h_0 is calculated as :

$$h_0 = 75 + 3 - 8 = 70 \text{ cm}$$

The design verification is based on the following flexural strength equation:

$$1 \times M_j \leq R_{ab'} \times (h_0 -) \gamma_s 2$$

Substituting the given values :

$$1 \times 216.314 = \times 14.3 \times 2.66 \cdot \times (0.70 -) \cdot 10^3 \quad 1.25 \quad 2 \times 216.314 = 30.4304 \times \times (0.70 -) \cdot 10^3 \quad 2$$

$$\times^2 \quad 30430.4 \quad (0.70 \times -) = 216.314 \quad 2 \quad \times^2 \quad 216.314 \quad (0.70 \times -) = 2 \quad 30430.4 \quad \times^2 \quad (0.70 \times -) = 0.0071 \quad 2 \quad \times^2 -$$

$$0.70 \quad \times + 0.0071 = 0 \quad 2 \quad \times^2 - 1.40 \times + 0.0142 = 0$$

Use quadratic equation formula : $x = (-b \pm \sqrt{b^2 - 4ac}) / 2a$

$$\sqrt{(1.402 - 4 \times 1 \times 0.0142)} \quad \times = (1.40 \pm) / 2 \times 1 \quad 1.380 \quad \times = (1.40 \pm) / 2 \times 1 \quad 1.40 - 1.380 \quad \times = () = 0.010$$

m, so $x = 0.010 \text{ m}$

This is given from the formula:

$$R_g A_g = R_{ab'} \quad \times$$

$$14.3 \times 2.66 \times 0.010 \quad A_g = = 11.53 \times 10^{-4} \text{ m}^2 = 11.53 \text{ cm}^2 \quad 330$$

6Φ16 steel bars are selected, $A_g = 12.06 \text{ cm}^2$

The flexural reinforcement is arranged in multiple layers. The center of the bottom layer of steel bars is positioned 5 cm above the beam's bottom edge, the vertical distance between the two layers of reinforcement is 6 cm. Accordingly, the effective concrete cover is :

$$a = 5 + 3 = 8 \text{ cm}$$

Based on this , functional depth of section measures calculated as follows :

$$h_0 = 70 \text{ cm}$$

Then,

$$330 \times 10.05 \quad \times = = 0.872 \text{ cm} \quad 14.3 \times 266 \quad \xi_g \times h_0 = 0.55 \times 70 = 38.5 \text{ cm} \geq \quad \times = 0.872 \text{ cm}, \text{ so meet the requirements}$$

Checking of the section strength :

$$1 \times M_p = R_{ab'} \quad \times (h_0 -) \quad \gamma_c \quad 2 \quad 1 \quad 0.01057 \quad M_p = \times 14.3 \times 103 \times 2.66 \times 0.01057 \quad (0.70 -) \quad 1.25 \quad 2 \quad M_p =$$

$$223.46 \text{ kN} \cdot \text{m} \geq M_j = 204.232 \text{ kN} \cdot \text{m}$$

b) Negative moment reinforcement

Using $a = 3 \text{ cm}$, $h_0 = 75 - 3 = 72 \text{ cm}$

$$1 \times M_j \leq R_{ab'} \quad \times (h_0 -) \quad \gamma_s \quad 2 \quad 1 \quad \times 18.56 \leq \times 14.3 \times 0.20 \times \times (0.70 -) \cdot 10^3 \quad 1.25 \quad 2$$

Then, $x = 0.012 \text{ m}$

This is given from the formula:

$$R_g A_g = R_{ab'} \quad \times 14.3 \times 0.20 \times 0.012 \quad A'_g = = 10.4 \times 10^{-5} \text{ m}^2 = 1.04 \text{ cm}^2 \quad 330$$

5φ16 steel bars are selected, $A' g= 10.05 \text{ cm}^2$, and then :
 $330 \times 10.05 \chi = = 11.60 \text{ cm}$ 14.3×20
Checking of the cross section strength :
 $1 \times M_p = Rab' \times (h_0 -) \gamma_c 2 1 0.1160 \text{ Mp} = \times 14.3 \times 103 \times 0.20 \times 0.1160 \times (0.72 -) 1.25 2 M_p =$
 $175.70 \text{ kN} \cdot \text{m} \geq 18.56 \text{ kN} \cdot \text{m}$
3) Checking calculation of cross section reinforcement :
 $24.63 \mu 1 = \times 100\% = 0.430\%$ $(266 \times 20) + (20 \times 20) 1.005 \mu 2 = \times 100\% = 0.697\%$ 20×72
Both μ land $\mu 2$ exceed the minimum required reinforcement ratio for tensile steel bars, as specified in the code, which is 0.15%.

| 指 标 | |
|---|-----------------------|
| 疑似剽窃文字表述 | |
| 1. In which: | |
| C1 : Consider coefficient of steel bar surface shape for threaded steel bars | $C1 = 1.0$ |
| C2 : Consider the coefficient of load action, long-term load action | $C2 = 1 + 0.5M_0 / M$ |
| Where M_0 represents the bending moment caused by long-term loading, while M denotes the bending moment experienced under the full-service load conditions. | |
| C3 : A coefficient relate to the form of a member, when a flexural member has a web | $C3 = 1.0$ |
| d : Diameter of the longitudinal tensile bar | A_g |
| μ : The ratio of reinforcement is calculated according to the following formula: | |
| 2. $i - b)h_i$ | |
| b_i, h_i : Width and thickness of tension flange | |
| σ_g : Stress of a tensile steel bar under service load, calculate according to the formula : | |
| $M \sigma_g = 0.87A_g h_0$ | |
| The following calculation evaluates whether the maximum crack width in the main beam span, under normal environmental conditions and 1 | |
| 3. nsidering the defined stiffness characteristics of the member. | |
| For simply supported beams : | |
| $5ML^2 / f = 0.85EI_0$ | |
| In the formula : | |
| L : Calculate | |
| 4. harmony. | |
| Chapter 5 Calculations of Diaphragm | |
| 5.1 Calculation of diaphragms | |
| In a reinforced concrete beam bridge that does not include tr | |
| 5. 3.82 kN/m $L \pi 3.1416$ | |
| 5.2 Bending moment calculations of diaphragm | |
| According to the calculation results shown in Table 5.1, influence line diagram for the transverse beam be | |
| 6. ed loads are arranged according to the most unfavorable loading configuration in the horizontal direction, presented in Figure 5.2. | |
| Given that the span length of the beam is 21.5 meters and the dynamic impact coefficient $1 + \mu = 1.276$, the bending moment at the mid-span section of the transverse beam, under various loading condition | |
| 7. 56 kN/m | |
| Accordingly, the resulting internal forces in the beam are : a) The positive bending moment is governed by the Highway - Grade I loading : | |
| $M(+)= 216.314 \text{ kN/m}$ | |
| b) The negative bending moment is gover | |
| 6. Scheme design and calculation of Liuquan Medium bridge on Rongwu highway_第6部分 | 总字数: 16388 |
| 相似文献列表 | |

| | | |
|---|---|-----------------------|
| 去除本人文献复制比： 5.8%(950) 去除引用文献复制比： 5.8%(950) 文字复制比： 5.8%(950) 疑似剽窃观点： (0) | | |
| 1 | Scheme Design and Structural Calculation of Chayuan middle-span bridge on Rongwu Highway NAURA BERLIAN HUMAIROH - 《大学生论文联合比对库》 - 2024-06-14 | 4.9% (798) 是否引证： 否 |
| 2 | Design of composite tidal turbine blades D.M. Grogan;;S.B. Leen;;C.R. Kennedy;;C.M. Brádaigh - 《英文比对库》 - 2013-09-15 | 0.5% (82) 是否引证： 否 |
| 3 | 15 Hongchen Liu_Study on digital twin technologies for Watershed Information Modeling (WIM)_ A s Hongchen Liu - 《大学生论文联合比对库》 - 2023-05-09 | 0.5% (77) 是否引证： 否 |
| 4 | Scheme design and calculation of Wangcun Middle-span bridge on Rongwu freeway M. FAREL ASHROFIE - 《大学生论文联合比对库》 - 2024-06-26 | 0.4% (70) 是否引证： 否 |
| 5 | An experimental study on the effect of environmental exposures and corrosion on RC columns with FRP composite jackets Abdeljelil Belarbi;;Sang-Wook Bae - 《英文比对库》 - 2006-06-15 | 0.4% (70) 是否引证： 否 |
| 原文内容 | | |

5.4 Shear force calculation and reinforcement design of the diaphragm

To compute the shear force on the diaphragm, the influence line for the transverse load distribution of the main beam is established using the eccentric pressure method. The shear force typically has the maximum value in the vicinity of the bridge edges. Therefore, it is considered sufficient to compute shear stress on the right part regarding main beams number 1 and number 2.

As per this procedure, the shear influence lines for such members are obtained. The shear influence line value at the right end of main beam number 1 is computed as follows : a) When a load of P = 1 is introduced, and the section is analysis to the left :

$\eta_{l0il} = \eta_{li} - 1$

b) When a load of P = 1 is introduced, and the section is analysis to the right :

$\eta_{l0il} = \eta_{li}$

For the right section of main beam number 1, the vertical ordinate of the shear influence line is describe as : a) When a load of P = 1 is introduced, and the section is analysis to the left :

$\eta_{l0i2} = \eta_{li} + \eta_{2i} - 1$

b) When a load of P = 1 is introduced, and the section is analysis to the right :

$\eta_{l0i2} = \eta_{li} + \eta_{2i}$

By the above step, the shear influence lines of the critical sections of main beams number 1 and number 2 are obtained, according to the most unfavorable position of loads corresponding to Highway Grade I load arrangement.

The figure below depicts the most critical positioning of the Highway Grade I load on the respective influence line, from which the sectional shear load is determined.

Shear load acting on right section of main bema number 1 due to the applied load is :

$Q_{q1} = (1 + \mu)P_q \sum \eta_q \times a$ $Q_{q1} = 1.276 \times 14.62 \times (0.533 + 0.333 + 0.189 - 0.011) \times 4.85$ $Q_{q1} = 94.46$ kN

Shear force of the right section number 2 main beam under the load :

$Q_{q2} = (1 + \mu)P_q \sum \eta_q \times a$ $Q_{q2} = 1.276 \times 14.62 \times (0.550 + 0.300 + 0.119 - 0.131) \times 4.85$ $Q_{q2} = 75.82$ kN

Based on the analysis outcomes, the shear force observed in the right segment of the main beam number 1, subjected to automobile loads is the most significant. Thus, the design shear force is considered to be:

$Q_{max} = 1.4 \times (Q_{q1}, Q_{q2})$ $Q_{max} = 1.4 \times (94.46, 75.82)$ $Q_{max} = 1.4 \times 94.46 = 132.24$ kN

Shear checking according to the standard:

$0.051 \sqrt{R_{bh0}} = 0.051 \times \sqrt{30 \times 20 \times 75} = 419.01$ kN $0.038 R_{bh0} = 0.038 \times 1.43 \times 20 \times 75 = 81.51$ kN

Since the computed force Qj = 130.44 kN lies between these two limits, it is concluded that shear reinforcement is required.

Assuming that the shear reinforcement consists entirely of stirrups, and using a single-leg stirrup of diameter $\phi 8$, the stirrup' s cross-sectional area is determined as illustrated.

$A_{gk} = 2 \times 0.503 = 1.006$ cm²

When the shear resistance of concrete and stirrup in inclined section is combined, the shear resistance is calculating according as shown :

$Q_{hk} = 0.0349 bh_0 \sqrt{(2 + P)} \sqrt{R} \mu k R_{gk}$

In this formula :

$A_g 10.05 P = 100 \mu = 100 \times = 100 \times = 0.67$ bh0 20 $\times 75$

Because :

$$Agk \mu k = bSk$$

So:

$$Agk Sk = b \mu k (0.0349)^{2b} h^{0.2(2+P)} \sqrt{R} Rgk Agk Sk = (Qhk)^2 0.00122 \times 20 \times 752 \times (2 + 0.67) \times \sqrt{30} \times 330 \times 1.006 Sk = 39.16 \text{ cm } 130.442$$

So take : $Sk = 39 \text{ cm}$, and then :

$$Agk \mu k = bSk$$

$$1.006 \mu k = 0.129\% \geq \mu k_{\min}, 20 \times 39.16$$

So meet the construction requirement of the specification.

Chapter 6 Special Research Transformation Medium-Span Bridge Design Through Advanced Materials and Digital Technologies for Sustainable Infrastructure

6.1 Scientific Rationale and Innovative Context

The paradigm shift in medium-span bridge design is characterised by the strategic integration of advanced materials and digital technologies, which have emerged as a scientific response to the global need for infrastructure that is adaptive, highly resilient, and orientated towards long-term sustainability. Innovative materials such as Ultra High Performance Concrete (UHPC), superior grade steel, and polymer composites reinforced with fibers have demonstrated substantial improvements in enhancing the load bearing capacity, corrosion durability, and longevity of bridge elements. The contributions of these materials can open up space for the development of leaner, lighter, and more energy-efficient structural forms. Alongside these technological developments, digital tools like Building Information Modelling (BIM) are also utilized, Digital Twin, and Structural-Health Monitoring (SHM) enable the creation of data-driven, and predictive infrastructure design and management systems. The Integration of these two aspects not only supports efficiency during the design and construction phase and optimisation of the life cycle of infrastructure assets (Torzoni et al., 2023; Tezzele et al., 2023).

Globally, a sustainability-based approach to bridge design has become an integral part of infrastructure development strategies, with the application of integrative models such as BIM combined with Life Cycle Sustainability Assessment (LCSA). This approach establishes framework for evaluating the impact of infrastructure project on environment, society, and economy during the entire lifespan of a bridge, thus encouraging more holistic and transdisciplinary decision-making. In China, implementation of this approach has shown results, such as research conducted by Zhou and Zhang (2020) identified a significant shift from a passive adoption model of technology towards domestic innovation in the bridge industry. A future study on the Xiamen Second Bridge, for example, showed drastically improved efficiency in project planning, supervision, and control through the full adoption of BIM (Meng et al., 2023).

The transformation of bridge design through advanced materials and digital technology is now seen as an innovative foundation in the development of future resilient infrastructure. In the policy and institutional context, support is needed through harmonisation of international standards, strengthening human resource capacity through digital engineering training, and innovation-oriented research investment across sectors. Increasing workforce readiness and expanding technical regulations will accelerate the penetration of these technologies into civil engineering practice at large. In a more strategic setting, collaboration between academics, practitioners, and regulators is the main catalyst for realising a medium-span bridge design system that is not only efficient and adaptive to climate challenges and dynamic traffic loads, but also contributes significantly to sustainable development goals on a global scale.

6.2 Innovative Materials in Medium Span Bridge Design

Use of innovative materials has revolutionised the design of mid-span bridges, allowing for lighter, more durable and energy efficient structures.

6.2.1 Ultra High Performance Concrete (UHPC)

Represents a specialized category of concrete material with high strength that shows significantly elevated compressive strengths, between 120 – 250 MPa, as well as exceptional resistance to corrosion, wear and influence of harmful substances. The usage of UHPC enables the design of slimmer and lighter structural elements without compromising on strength or durability.

Research by Xu et al. (2023) states that the addition of silica fume in UHPC mixes, combined with thermal curing, significantly increases the compressive strength and improves the microstructure of concrete. These results indicate the potential of UHPC in producing structures that are denser, impermeable, and resistant to aggressive environments.

In addition, a study by Rahat Ullah et al. (2022) states that UHPC has very low porosity, thus providing high resistance to chloride attack and carbonation—this makes UHPC a very suitable material for long-term infrastructure applications, including bridges, especially in the context of sustainability and maintenance efficiency.

6.2.2 Fibre Reinforced Polymers (FRP)

Composite polymer materials reinforced with fibers, notably Glass Fibre Reinforced Polymers (GFRP) and Carbon Fibre-Reinforced Polymer (CFRP), exhibit high structural efficiency and resistance to corrosion, making them a viable alternative to bridge reinforcement and retrofitting.

According to Kossakowski and Wcislik (2022), FRP has several key advantages in bridge construction, including:

- 1) Superior mechanical parameters : FRP has a higher tensile strength than conventional structural steel, allowing a reduction in structural weight without sacrificing strength.
- 2) Resistance to corrosion : FRP is highly resistant to aggressive environments, including chemicals and alkalis, which increases the durability of the bridge structure.
- 3) Minimal maintenance : FRP structures require less maintenance compared to steel or concrete structures, which reduces long-term maintenance costs.
- 4) Free-forming capability : FRP manufacturing technology allows the formation of bridge elements with complex and specialised shapes, which are difficult to achieve with conventional materials.

Research conducted by Zakkaria and Shanmugam (2023) demonstrated that incorporating GRFP as reinforcement in reinforced concrete beams enhances flexural strength and minimizes crack widths, particularly in aggressive marine environments. The addition of polypropylene fibres in concrete also contributes to improved crack resistance and durability of the structure.

6.2.3 High-Strength Steel (HSS)

Application of HSS in building medium spans bridges, this approach has become the key strategy for enhancing structural performance while minimizing environmental effects. The characteristics of High Strength Steel (HSS) that allow the manufacture of structural elements that are thinner and lighter, but must remain strong, to be an important factor in reducing the amount of material required and emphasising the carbon footprint during the operational life of the bridge.

Research results from Lu et al. (2024) stated that the use of Q690qE steel showed outstanding resistance to corrosion fatigue under artificial marine environment conditions. This makes it a very cool material for bridge components that must withstand repeated loads over an extended period, thereby increasing protection and extending service life of the structure.

In addition, according to Al-Karawi et al. (2023) stated that the High Frequency Mechanical Impact (HFMI) technique proved effective in improving the durability of welded joints of HSS steel against structural fatigue. The application of this method notably improved the durability of weld joints, which are often considered weak spots in steel structures.

Meanwhile, the steel industry in China has experienced rapid development in the production of localised HSS such as HRB500 and HRB600. Increasing the domestic high-quality steel production capacity not only strengthens the industry's self-reliance, but also spurs technological innovation in the country's modern bridge construction.

Table 6. 1 Material Comparisons : UHPC - FRP - HSS

| Technical |
|---------------------------------|
| UHPC |
| Properties |
| Compressive |
| 150 - 200 MPa |
| strength |
| Tensile strength 7 - 15 MPa |
| Corrosion |
| Very strong |
| resistance |
| Bulk weight |
| ~2.5 g/cm³ |
| Life of service |
| >100 Years |
| Ductility |
| Low (brittle) |
| Deck, joint, |
| Application ideal prefabricated |
| structure |
| Cost |
| High |
| Construction High precision, |
| process |
| needs curing |
| Limited, |
| Availability in |
| increased in |
| Asian market |

China & Korea
FRP
HSS (Q690/Q890)
(Carbon/GRFP)
~600 - 1200 MPa
690 - 890 MPa
(Tensile strength)
600 - 1500 MPa 600 - 750 MPa
Very strong
Medium
1.6 - 2.0 g/cm³
~7.85 g/cm³
>50 Years (with
50 - 75 Years
UV protection)
High (flexible)
High
Reinforcement of Main structure,
beams, tendons, stay
compact
cables
columns/beams
Medium - high
Medium
(depending on type)
Easy, fast
Conventional
installation
Widely available in
Widely imported,
China & Southeast
limited local
Asia

6.3 Integration of Digital Technologies in Bridge Engineering

Digital technology has a significant role in advancing the modernization of a bridge and management, enabling a more efficient and sustainable approach.

6.3.1 Building Information Modelling (BIM)

Building Information Modelling (BIM) refers technology that enables representation of physical and functional information of structures in the form of integrated digital models. BIM supports various stages in the life cycle of infrastructure projects, from planning and design to construction and maintenance. By integrating BIM into Life Cycle Sustainability Assessment (LCSA), that technology offers a framework to assess the sustainability of projects from environmental, social, and economic perspectives.

Li, Li, and Ding (2024) in their study titled “Exploring Building Information Modelling in Civil Infrastructure Study Covering 2020-2024” reported a significant increase in the adoption regarding the use of intelligent digital modelling systems in civil engineering infrastructure endeavors, including bridges, over recent years. It is highlighted that the implementation of intelligent digital construction modelling systems has evolved beyond the traditional phases of design and planning. At present, BIM is increasingly merged with state of art innovations like AI and IoT systems to support the monitoring and evaluation of structural performance. This supports faster and more precise decision-making in bridge maintenance and repair, which improves infrastructure management efficiency (Li, Li, & Ding, 2024).

This research also proves that the use of BIM is essential in accelerating the construction process and optimising the use of resources in large bridge projects. With better data management and more accurate visualisation, BIM also enables more efficient design, reduces waste, and improves project sustainability. BIM is also used as an integrated tool to assist in smarter decision-making throughout the infrastructure lifecycle, including bridge maintenance, leading to reduced long-term maintenance costs.

6.3.2 Digital Twin (DT)

DT is a technology that connects the physical world and the digital world through a digital model of a physical object that is continuously updated to reflect its current state. Within the context of bridge management, the application of a Digital Twin allows for more accurate and efficient structural condition monitoring on an ongoing basis. Data collected by sensors can be directly integrated into the digital model,

which helps in detecting potential damage much earlier. DT therefore supports a predictive maintenance approach that not only reduces maintenance costs but also extends the operational life of the bridge. In addition, DT has the ability to simulate load scenarios and contextual influences, which provides an additional advantage for better bridge maintenance planning.

In research conducted by Hagen and Anderson (2024), the application of Digital Twin (DT) the applications in bridge structure was illustrated by a case study of the

Stava Bridge in Norway. In this project, DT was used to monitor the condition of the bridge using data collected by Internet of Things (IoT) sensors. When significant structural damage was detected, DT enabled early identification of the problem and virtual analysis of the condition. This is critical to support informed decision-making for maintenance and prevention of further damage, optimising time and resources.

In addition, research conducted by Torzoni (2023) also developed a probabilistic model-based Digital Twin (DT) framework for structural health monitoring and bridge maintenance planning. This model integrates sensor data with deep learning technology to provide diagnosis of bridge conditions. Using this information, maintenance planning can be performed more optimally, prioritising based on the level of damage and needs identified from the available data.

However, Implementation on (DT) challenges remain in bridge management a number of technical challenges, including limited interoperability between digital platforms, complexity in processing big data, and the development of more efficient IoT-based anomaly detection models.

6.3.3 Structural Health Monitoring (SHM)

Structure Health Monitoring (SHM) is a technological approach used to continuously monitor bridge conditions by acquiring data from various sensors embedded in the structure. It also contributes to early damage detection, structural integrity evaluation, and data driven maintenance decision making.

SHM systems generally consist of several main components, namely:

| 指 标 | |
|---|------------|
| 疑似剽窃文字表述 | |
| <div>1. To compute the shear force on the diaphragm, the influence line for the transverse load distribution of the main beam is established using the eccentric pressure method. The shear force</div> <div>2. = 2 × 0.503 = 1.006 cm2</div> <div>When the shear resistance of concrete and stirrup in inclined section is combined, the shear resistance is</div> | |
| 7. Scheme design and calculation of Liuquan Medium bridge on Rongwu highway_第7部分 | 总字数: 14347 |
| 相似文献列表 | |
| 去除本人文献复制比: 1.1%(160) 去除引用文献复制比: 1.1%(160) 文字复制比: 1.1%(160) 疑似剽窃观点: (0) | |
| 1 大型桥梁结构健康监测系统云平台设计与实现 | 0.6% (89) |
| 黄旭 - 《大学生论文联合比对库》 - 2024-06-16 | 是否引证: 否 |
| 2 Review and discussion on structural health monitoring in civil engineering | 0.5% (71) |
| MD SAJIB SARKAR - 《大学生论文联合比对库》 - 2023-06-14 | 是否引证: 否 |
| 原文内容 | |

1) Physical sensors : Such as strain gauges, accelerometers, displacement sensors, and temperature sensors.

2) Data acquisition unit (DAQ) : Serves to collect and transmit data from sensors to the processing centre.

3) Analysis and modelling software : Used to analyse changes in structural characteristics, such as natural frequency, deformation, or vibration, as an indicator of structural degradation.

4) Communications network : Enables remote and automated monitoring

These components are integrated with each other to provide a monitoring system that is accurate and adaptive to structural dynamics due to traffic loads and environmental influences.

SHM has been widely implemented in bridge projects in various countries, especially in long bridge structures, arch bridges, and structures exposed to high dynamic loads. The sensors are installed in critical parts of the structure such as joints, main pillars, and decks, which are most susceptible to material fatigue. The implementation of SHM is also highly relevant for bridges integrating innovative compounds, such as ultra durable concrete variants, fiber enhanced polymer composites, and steels with elevated strength characteristics, as it enables continuous monitoring of new materials.

6.4 Case Study : Implementation in China

6.4.1 Project Xiamen Second East Passage

The Xiamen Second East Passage project is one example of the application of advanced technology in the bridge infrastructure sector in China that fully integrates Building Information Modelling (BIM) utilization of technology starting from the early design process to construction execution. Zhang et al. (2023), indicated that the integration of BIM systems within the project notably enhanced the effectiveness of technical design processes, ensured better control over construction quality, and contributed positively to the overall coordination and management of the project. The technology enabled three-dimensional visualisation of the bridge structure, early detection of design conflicts, and optimisation of the project schedule through digital simulation (4D scheduling).

The project also implemented a technology based management platform built upon networked sensing technologies and intelligent computational systems to monitor structural performance. According to Liu and Chen (2023), this system enables post-construction evaluation of structural conditions using smart sensors embedded in key bridge elements, such as prestressing cables and expansion joints.

The implementation of these advanced technologies significantly accelerates the process of construction workflow while simultaneously enhancing precision and safety the project. For example, the use of prefabricated segmental bridge elements that are manufactured with high precision in a factory and assembled at the construction site helps to reduce site work time and minimise the risk of human error (Wang et al., 2024).

With the integration of BIM technology, IoT, and prefabricated systems, the Xiamen Second Bridge project became a landmark case in the adoption of digital technology and advanced materials in China's construction industry. This aligns with the global movement toward smart and sustainable infrastructure development, and may also serve as a valuable model for developing nations seeking to adopt comparable strategies.

6.4.2 Hong Kong - Zhuhai - Macau Bridge (HZMB)

Hong Kong - Zhuhai - Macau Bridge (HZMB) is widely regarded as one of the largest and most complex civil engineering projects ever developed on a global scale, this project spans over 55 km in length. It serves as a connection between the autonomous administrative zones of Hong Kong and Macau and mainland Zhuhai, a coastal municipality in southern China. In construction process, a combination of cable-stayed structures, undersea tunnels, and two artificial islands were used. The project was designed to enhance regional connectivity in the Pearl River Delta and support economic integration between the three regions.

In terms of construction materials, the project employed advanced engineering construction substances like ultra dense cementitious composites (commonly referred to as UHPC) and weather resistant high strength alloyed metal. Utilization on UHPC aims to improve the concrete's ability to resist chloride ion infiltration, a key factor contributing to reinforcement corrosion in marine environments, thereby extending structural resilience and operational lifespan. Corrosion-resistant steel, meanwhile, was used for the main structural elements to minimise long-term maintenance costs and provide protection against the extreme environmental conditions typical of coastal areas.

In terms of digital technology, the HZMB project implemented a comprehensive Building Information Modelling (BIM) approach integrated with a Geographic Information System (GIS). This integration enables precise and efficient spatial management, and facilitates coordination across administrative regions. BIM is used for a variety of purposes ranging from structural design planning, interference inspection between components, to monitoring construction progress. GIS, on the other hand, provides visualization. This is especially valuable for environmental monitoring and assessing the impacts of projects.

In addition, the project utilises the Digital Twin system, which is a digital representation of the bridge's physical condition connected to sensor data directly through Internet of Things (IoT) technology. This system allows simulation and monitoring of the actual condition of the bridge structure such as deformation, vibration, and corrosion levels. Such information is very useful in data-driven decision-making, especially for preventive maintenance and efficient long-term maintenance management.

The effective application of digital technology on the project proved to have a significant impact in terms of operational efficiency and cost savings. The use of BIM and Digital Twin (DT) was able to reduce the potential for design errors, speed up the coordination process between teams, and save up to 12% of the construction budget and reduce survey costs by 15%. This shows that the adoption of cutting-edge technology not only improves the durability of the structure, but also drives overall project economic efficiency.

6.5 Policy and Institutional Framework

The transformation of bridge design to integrate advanced materials and digital technologies requires strong policy and institutional support. This includes harmonising international standards, strengthening human resource capacity, and investing in research across sectors.

6.5.1 Harmonising international standards

In the era of globalisation of infrastructure development the need for harmonised international standards is becoming increasingly urgent, especially in the context of material specifications and the integration of digital engineering systems. A major challenge in applying digital twin technology to bridge projects is the lack of a well-defined and organized global standards framework. The inconsistency in terminology as well as

implementation approaches leads to variations in results, which impacts the overall effectiveness of the technology. Hence, there is pressing need for collaborative international efforts to establish standardized guidelines that encompass every phase of a bridge's lifecycle including planning, design, construction, and the management of operation and maintenance activities (SAGE Journals, 2023).

In China, similar challenges are also found in the digital transformation process of the construction sector. The absence of uniform technical standards has been a major obstacle to the systematic application of digital technologies. To overcome this obstacle, Chinese institutions have been pushing for the development and implementation of comprehensive national technical standards, hoping to align with international practices and support cross-border collaboration on large multinational projects (MDPI, 2024).

Overview of strategic issues in international standards harmonisation:

- 1) The disharmony of global technical standards is a major obstacle to the application of digital technologies, including the digital twin, in the internationally orientated bridge engineering sector.
- 2) The variation in definitions and implementation approaches of the digital twin leads to inconsistencies in the quality and effectiveness of the technologies applied to various infrastructure projects.
- 3) There is an escalating need for the standardization of global regulations to ensure consistency across all phase of the bridge lifecycle, from design through to maintenance.
- 4) The unavailability of adequate national technical standards in China is a major constraining factor in the digital transformation of the construction sector, despite the country's strong commitment to technological modernisation.
- 5) Intensive international collaboration between stakeholders from academia, industry, and government is needed to develop standards that are universal, adaptive, and applicable across jurisdictions.

6.5.2 Strengthening human resources capacity

Digital transformation in the construction sector, especially in bridge design and construction, requires Human Resources (HR) competent in advanced innovations such as BIM, Digital Twin, and sensor-based systems. However, there is still a significant shortage of labour with adequate digital skills, especially in China, which hinders the digital transformation process of the construction industry.

To address this challenge, intensive and continuous training programmes designed to improve the digital skills of the workforce are required. In addition, strategies to attract and retain digital talent are also important, including competitive incentives, clear career path development, and a work environment that supports innovation. Incorporation of digital tools and systems in training, for example use on the Digital Twin (DT) platform and Virtual Reality (RV), has proven effective in improving training efficiency and the workforce's practical understanding of construction projects has increased employee training efficiency by 60%. In addition, the use of VR in bridge inspection training enables realistic simulation of field conditions, improving the readiness and technical skills of the workforce.

To overcome this challenge, strengthening human resource competencies through structured training programs and the integration of digital technologies is considered a vital approach to support successful deployment of digital solutions in the building process industry, especially in the areas of bridge construction and maintenance.

6.5.3 Investment in cross-cutting research

The development of intelligent bridge technology in the digital age requires significant investment in cross-sector research, involving collaboration between academics industry practitioners, and policy makers. In China, initiatives such as "Bridge 2025" emphasize the importance of integrating advanced computational technological advancements including IoT (Internet of Things), the analysis of large scale datasets, and cloud based computing systems into development also innovation on intelligent bridge systems. Programme includes research projects focusing on the construction and management of intelligent bridges, as well as the development of integration platforms for construction and maintenance.

Furthermore, global forums like BDIOT 2025 and ICBAIE 2025 serve as key venues for academics and industry professionals to disseminate recent research findings and foster collaborative efforts on areas covering massive data management, IoT frameworks, and AI driven applications.

Investment in cross-sector research also includes the development of intelligent bridge management systems through big data-based knowledge engineering. This approach enables more efficient and predictive bridge maintenance, and improves the safety and reliability of the infrastructure. This makes continued investment in cross-sector research key to driving innovation and improving the competitiveness of the bridge industry in the digital age.

REFERENCE

- [1] (Ministry of Transport of the People's Republic of China, 2015). Specifications for the design of highway and culverts (in Chinese). Beijing: China Communications press.
- [2] (Ministry of Transport of the People's Republic of China, 2018). Code for the design of highway reinforced and prestressed concrete bridges and culverts (in Chinese). Beijing: China Communications Press.
- [3] (Jianguo, Yi, 2020). Bridge Calculation Example Series-Concrete Simply Supported Girder (Slab) Bridge. Beijing People's Traffic Press.

- [4] (AASHTO, 2012). Bridge design specifications based on load and resistance factor design (LRFD), units C.
- [5] (Highway Bridge and Culvert Design Manual - Girder Bridges (Upper Volume). press, People traffic, 1998)
- [6] Ye Mishu, edited by Ye Mishu (Mishu, 2020), 2020. Principles of Structural Design. Beijing : People's Transportation Press
- [7] Yuan Lunyi and Bao Weigang, " (Weigang, 2004), Example of Application of Provisions. Beijing : People's Transportation Press, 2005. 3.
- [8] (Jootoo A. &, 2018) Bridge Type Classification: Supervised Learning on a Modified NBI Dataset.
- [9] (Cui, 2023). Discusses the effects of chloride ion erosion on pre-stressed concrete bridges located in cold climate regions.
- [10] (Pei, 2023). Optimization of Preventive Maintenance Timing of Highway Bridges Considering China's "Dual Carbon" Target.
- [11] (Li X. e., 2024) Finite Element Analysis of Steel Truss Bridge Structure Based on MIDAS.
- [12] (Li H. e., 2024), Shape memory alloy-reinforced UHPC tube confined bridge piers for enhancing the seismic resistance of highway bridges.
- [13] (Wang, 2024), Vibration control of corrugated steel web box girder bridge with friction pendulum isolation.
- [14] (Kang, 2024), Accelerated Bridge Construction Case: A Novel Low-Carbon and Assembled Composite Bridge Scheme.
- [15] (Wang, K., 2025), Study on comprehensive evaluation and decision-making method for all-composite bridge structure design scheme.
- [16] (Samtani, N. C., & Kulicki, J. M., 2022), Structural Considerations and Implications Related to Foundation Movements in AASHTO LRFD
- [17] (National academies of science, engineering, and medicine, 2010), LRFD Design and Construction of Shallow Foundations for Highway Bridge Structures. Washington
- [18] (Gavin, K., & Lehane, B., 2019), Comparison of Canadian Highway Bridge Design Code and AASHTO LRFD bridge design specifications regarding pile design subject to negative skin friction.
- [19] (Kromoser, B., & Kolleger, J., 2021), Semi-precast segmental bridge construction method
- [20] (Yazici, H., & Arel, H. S., 2023), Performance evaluation of high-performance self-compacting concrete incorporating recycled materials.
- [21] (Zhang, X., & Wang, Y., 2023), Integration of building information modelling and project management in construction project life cycle.
- [22] (Zhou, X., & Zhang, X., 2019), Thoughts on the development of bridge technology in China
- [23] (Kossakowski, P., & Weislik, M., 2022), Fibre-Reinforced Polymer Composites in the Construction of Bridges.
- [24] (Al-Karawi, H., et al., 2023), Verification of the maximum stresses in enhanced welded details via high-frequency mechanical impact in road bridges.
- [25] (Xu, D., et al., 2023), Influence of silica fume and thermal curing on long-term hydration, microstructure and compressive strength of UHPC.
- [26] (Meng, F., et al., 2023), Design and BIM-based technology on a new cross-sea bridge in Xiamen, China.
- [27] (Lu, C., et al., 2024), Corrosion fatigue cracking behaviours of Q690qE high-strength bridge steel.
- [28] (Torzoni, M., et al., 2024), A digital twin framework for civil engineering structures.
- [29] (Li, Y., et al., 2024), Building Information Modelling Applications in Civil Infrastructure: A Bibliometric Analysis from 2020 to 2024
- [30] Hagen, A., & Andersen, T. M. (2024). Digital Twins: Damage detection on reinforced concrete bridge. Wang, M., et al. (2024). The main bridge of Xiamen's Second East Passage. DF Prestress.
- [31] (BIM+, 2018), Bentley's BIM technology on Hong Kong-Zhuhai-Macao Bridge.
- [32] (Naji, K. K., et al., 2024), Assessing the digital transformation readiness of the construction industry.
- [33] (Ministry of Transport of the People's Republic of China., 2019), Specifications for Design of Foundation of Highway Bridges and Culverts (JTG 3363—2019).
- [34] (Yin, P., Yang, K., Zhao, M., He, W., & Zhang, Y., 2022), Determination Method for the Foundation Horizontal Resistance Ratio Coefficient Under Consideration of the Slope Effect. China Journal of Highway and Transport, 35(11), 12–20.
- [35] (Zhu, J., Qian, F., & Cai, J., 2024), Research on a Calculation Method for the Horizontal Displacement of the Retaining Structure of Deep Foundation Pits. Buildings, 14(6), 1694.
- [36] (Wang, J., Liu, S., et al., 2021), Corrosion resistance and mechanical properties of high-strength steel used in bridge construction. Materials, 14(3), 567.
- [37] (Zhang, L., Chen, X., et al., 2020), Enhancement of durability and sustainability in concrete bridges using fly ash and supplementary cementitious materials. Materials, 13(22), 5111.

ACKNOWLEDGEMENT

All praise and gratitude I extend to Allah SWT for abundant blessings, guidance, and mercy throughout my journey. With deep gratitude, I honor my father, Mr. Basri, an outstanding educator whose dedication enabled all his daughters to complete their undergraduate studies. I am also profoundly thankful to my mother, Mrs. Sri Mahdayeni, for her constant love and support. Special thanks go to my sisters, Dewi Permatasari and Ulfa Mayasari, and my extended family in Lubuk Linggau, for their continuous encouragement and care.

My sincere appreciation goes to all lecturers and academic staff at State Polytechnic of Sriwijaya, who have generously shared their knowledge and guidance throughout my studies in Indonesia. My deepest thanks go to Mr. Ir. Irawan Rusnadi, M.T., the Director, as well as to leadership of the Civil Engineering Department : Mr. Ibrahim, S.T., M.T., Mr. Ahmad Syafawi, S.T., M.T., Mr. Andi Herius, S.T., M.T., Mr. M. Sang Gumilar Panca Putra S.S.T., M.T., and Mr. Didi Yuda Wiranata, S.T., M.T. I am also truly grateful to Mrs. Dra. Tiur Simanjuntak, M.Ed.M., and Mrs. Dra. Nyayu Latifah Husni, S.T., M.T., of the International Programme staff, for their trust and guidance throughout my academic journey and for the opportunity to be part of this programme.

I sincerely thank Mr. Hu Xingyu, Head of State of Shandong University of Science and Technology, also my academic supervisors, Mrs. Yuying Jiao, for her ongoing guidance valuable feedback during my final project and studies. I also appreciate Professor Yang X, Head of the Civil Engineering Department who oversees academic and research activities, along with all faculty members, for their important contributions to my learning. Special thanks to Mr. Henry Lee for facilitating my entry into the 2+2 Double Degree Programme, and to my counsellor Mrs. Zhou and the International College staff for their continuous support throughout my academic and administrative journey in China.

I warmly thank my dear friends Andini, Tiara, Lusiana, Silvi, Nanda, and Loly, whose support and encouragement have remained strong despite the distance. I also deeply appreciate Imelda, my classmate from Indonesia, for her invaluable help during the beginning of my studies. Additionally, I sincerely appreciate all my classmates for their assistance also friendship from PJJC and HMJ21 for their friendship and teamwork, which have made this journey truly unforgettable.

It has been privilege to lead the Indonesian Students Association at the Shandong Branch in China, an experience that expanded my knowledge and global connections. I am deeply grateful to all members for their trust. Especially my roommate and classmates Selvi, who supported me through many challenges and joys. Thanks also to classmates Hajar, Gaminda, Arnob, and Shanto for their camaraderie, and to my dorm mates Fildzah, Yesa, Shona, Salvira for bringing warmth and happiness to my daily life. Your support has truly made this journey unforgettable

Finally, I sincerely appreciate myself for persevering through every challenge encountered along this journey, embracing growth and staying resilient through both the highs and lows. This achievement is not an end, but a starting point for a new journey. I am committed to continuing my growth and becoming a better version myself moving forward.

Thankyou very much

Terimakasih banyak

说明：1. 总文字复制比：被检测论文总重合字数在总字数中所占的比例

2. 去除引用文献复制比：去除系统识别为引用的文献后，计算出来的重合字数在总字数中所占的比例

3. 去除本人文献复制比：去除作者本人文献后，计算出来的重合字数在总字数中所占的比例

4. 单篇最大文字复制比：被检测文献与所有相似文献比对后，重合字数占总字数的比例最大的那一篇文献的文字复制比

5. 复制比：按照“四舍五入”规则，保留1位小数

6. 指标是由系统根据《学术论文不端行为的界定标准》自动生成的

7. 红色文字表示文字复制部分；绿色文字表示引用部分（包括系统自动识别为引用的部分）；棕灰色文字表示系统依据作者姓名识别的本人其他文献部分

8. 本报告单仅对您所选择的比对时间范围、资源范围内的检测结果负责



✉ amlc@cnki.net

🌐 <https://check.cnki.net/>

ACKNOWLEDGEMENT

All praise and gratitude I extend to Allah SWT for abundant blessings, guidance, and mercy throughout my journey. With deep gratitude, I honour my father, Mr. Basri, an outstanding educator whose dedication enabled all his daughters to complete their undergraduate studies. I am also profoundly thankful to my mother, Mrs. Sri Mahdayeni, for her constant love and support. Special thanks go to my sisters, Dewi Permatasari and Ulfa Mayasari, and my extended family in Lubuk Linggau, for their continuous encouragement and care.

My sincere appreciation goes to all lecturers and academic staff at State Polytechnic of Sriwijaya, who have generously shared their knowledge and guidance throughout my studies in Indonesia. My deepest thanks go to Mr. Ir. Irawan Rusnadi, M.T., the Director, as well as to leadership of the Civil Engineering Department : Mr. Ibrahim, S.T., M.T., Mr. Ahmad Syafawi, S.T., M.T., Mr. Andi Herius, S.T., M.T., Mr. M.Sang Gumilar Panca Putra S.S.T., M.T., and Mr. Didi Yuda Wiranata, S.T., M.T. I am also truly grateful to Mrs. Dra. Tiur Simanjuntak, M.Ed.M., and Mrs. Dra. Nyayu Latifah Husni, S.T., M.T., of the International Programme staff, for their trust and guidance throughout my academic journey and for the opportunity to be part of this programme.

I sincerely thank Mr. Hu Xingyu, Head of State of Shandong University of Science and Technology, also my academic supervisors, Mrs. Yuying Jiao, for her ongoing guidance valuable feedback during my final project and studies. I also appreciate Professor Yang X, Head of the Civil Engineering Department who oversees academic and research activities, along with all faculty members, for their important contributions to my learning. Special thanks to Mr. Henry Lee for facilitating my entry into the 2+2 Double Degree Programme, and to my counsellor Mrs. Zhou and the International College staff for their continuous support throughout my academic and administrative journey in China.

I warmly thank my dear friends Andini, Tiara, Lusiana, Silvi, Nanda, and Loly, whose support and encouragement have remained strong despite the distance. I also deeply appreciate Imelda, my classmate from Indonesia, for her invaluable help during the beginning of my studies. Additionally, I sincerely appreciate all my classmates for their assistance also friendship from PJJC and HMJ21 for their friendship and teamwork, which have made this journey truly unforgettable.

It has been privilege to lead the Indonesian Students Association at the Shandong Branch in China, an experience that expanded my knowledge and global connections. I am

deeply grateful to all members for their trust. Especially my roommate and classmates Selvi, who supported me through many challenges and joys. Thanks also to classmates Hajar, Gaminda, Arnob, and Shanto for their camaraderie, and to my dorm mates Fildzah, Yesa, Shona, Salvira for bringing warmth and happiness to my daily life. Your support has truly made this journey unforgettable

Finally, I sincerely appreciate myself for persevering through every challenge encountered along this journey, embracing growth and staying resilient through both the highs and lows. This achievement is not an end, but a starting point for a new journey. I am committed to continuing my growth and becoming a better version myself moving forward.

Terimakasih banyak

致谢

摘要

本桥梁设计基于荣乌柳泉中桥的地质勘察数据，涵盖了方案比选、上部结构设计分析以及后期养护与维修策略的专项研究。设计工作的主要内容包括：

1. 设计参数：本桥按照一级公路荷载标准设计，桥面布置为双车道。抗震设防等级为 B 类，地基土层为粉质黏土。
2. 方案比选：对几种桥梁结构方案进行了评估，包括开放式拱桥，预应力空心板桥以及钢筋混凝土简支梁桥。通过全面的比较分析，最终确定钢筋混凝土简支梁桥为最佳方案。
3. 结构设计与分析：上部结构采用 T 型梁截面形式。设计内容包括纵向高程布置，通过横向荷载分布系数与荷载组合效应确定关键参数，以及钢筋的合理布置。对主梁进行内力分析，并验证其抗弯性能，抗剪能力以及挠度是否满足规范要求。此外，设计还包括横隔板布置，钢筋结构细节及桥面铺装连续性的详细计算。
4. 专题研究：基于深度学习算法的检测工具已被开发，用于识别桥面板上的裂缝。该技术通过自动化裂缝识别过程，显著提升了养护工作的准确性和效率。

关键词：公路桥梁简支 T 形梁，上部结构，内力计算，AutoCAD.

ABSTRACT

The bridge design is informed by geological data from the Liuquan Medium Bridge on Rongwu Highway and encompasses scheme selection, structural analysis for both the superstructure, as well as a focused study on maintenance and repair strategies. Major components of the design include :

1. Design Criteria : The bridge is designed to accommodate Class I Highway Loads and features two lanes. The seismic design falls under category B, with a foundation layer composed of silty clay.
2. Scheme Evaluation : Several bridge structure alternatives were evaluated, such as the open spandrel arch type, the prestressed hollow slab design, and the simply supported beam bridge utilizing reinforced concrete. Following a thorough comparison, the reinforced concrete beam bridge was determined to be most effective and suitable choice.
3. Structural Design and Analysis : The T-beam cross-sectional form is adopted for the superstructure configuration. The design process encompasses vertical alignment planning, the calculation of critical design parameters through lateral load distribution coefficients and load combination effect, as well as a systematic arrangement of reinforcement bars. Structural analysis was conducted to assess internal forces acting on the main beams, followed by validation of flexural strength, shear resistance, and deflection compliance. Furthermore, the design integrates thorough calculations related to diaphragm placement, reinforcement detailing, and surface layer continuity.
4. Special Research : A software application utilizing deep learning algorithms has been developed to facilitate the detection of surface cracks on bridge decks. By automating the crack detection process, this technology significantly improves the precision and effectiveness of maintenance activities.

Keywords : Highway bridges Simply Supported T-beam, Superstructure, internal force calculation, AutoCAD.

TABLE OF CONTENTS

| | |
|--|-----------|
| 摘要..... | i |
| ABSTRACT..... | ii |
| Chapter 1 Overview of Bridge Design | 1 |
| 1.1 Project Overview | 1 |
| 1.2 Design basis and main design specification..... | 1 |
| 1.3 Design technical standards..... | 2 |
| 1.4 Design Essentials | 2 |
| Chapter 2 Theoretical and Structural Design of Bridges..... | 4 |
| 2.1 Introduction..... | 4 |
| 2.2 Bridge Design Concepts | 5 |
| 2.2.1 Classification of Bridge | 5 |
| 2.2.2 Material Selection in the Bridge Construction..... | 6 |
| 2.3 Geological Condition | 7 |
| 2.4 Plan Comparison..... | 9 |
| Chapter 3 Calculation of the Reinforced Concrete T-Beam | 12 |
| 3.1 Design Data and Structural Layout..... | 12 |
| 3.1.1 Design Data..... | 12 |
| 3.1.2 Design of Carriageway Slab | 13 |
| 3.1.3 Dead Load Internal Force | 14 |
| 3.1.4 Live load internal force | 14 |
| 3.1.5 Combination of internal force | 17 |
| 3.2 Reinforcement Design | 17 |
| 3.2.1 Reinforcement at fulcrum | 17 |
| 3.2.2 Reinforcement at Mid-span..... | 18 |
| 3.3 Calculation of connecting reinforcement..... | 20 |

| | | |
|---|--|-----------|
| 3.3.1 | Calculation effect of flexural member | 20 |
| Chapter 4. Design and Calculation of Main Beam | | 23 |
| 4.1 | Internal forces due to dead load are analysis | 23 |
| 4.2 | Calculation of internal forces under live load..... | 26 |
| 4.3 | Reinforcement design and strength checking calculation..... | 41 |
| 4.3.1 | Principal longitudinal reinforcement arrangement | 41 |
| 4.3.2 | Arrangement of shear reinforcement | 43 |
| 4.3.3 | Crack Verification Calculations | 53 |
| 4.3.4 | Main beam deflection verification calculation | 54 |
| Chapter 5 Calculations of Diaphragm | | 56 |
| 5.1 | Calculation of diaphragms | 56 |
| 5.2 | Bending moment calculations of diaphragm | 58 |
| 5.3 | Strength and reinforcement verification of diaphragm..... | 60 |
| 5.4 | Shear force calculation and reinforcement design of the diaphragm..... | 64 |
| Chapter 6 Special Research | | 66 |
| 6.1 | Scientific Rationale and Innovative Context | 66 |
| 6.2 | Innovative Materials in Medium Span Bridge Design | 67 |
| 6.2.1 | Ultra High Performance Concrete (UHPC) | 67 |
| 6.2.2 | Fibre Reinforced Polymers (FRP) | 67 |
| 6.2.3 | High-Strength Steel (HSS)..... | 68 |
| 6.3 | Integration of Digital Technologies in Bridge Engineering..... | 69 |
| 6.3.1 | Building Information Modelling (BIM)..... | 69 |
| 6.3.2 | Digital Twin (DT) | 70 |
| 6.3.3 | Structural Health Monitoring (SHM)..... | 71 |
| 6.4 | Case Study : Implementation in China | 72 |
| 6.4.1 | Project Xiamen Second East Passage | 72 |
| 6.4.2 | Hong Kong – Zhuhai – Macau Bridge (HZMB) | 73 |

| | |
|--|----|
| 6.5 Policy and Institutional Framework..... | 74 |
| 6.5.1 Harmonising international standards | 74 |
| 6.5.2 Strengthening human resources capacity | 75 |
| 6.5.3 Investment in cross-cutting research..... | 75 |
| REFERENCE..... | 77 |
| AKNOWLEDGEMENT | 86 |